5034

Final Report

THE USE OF LANGMUIR PROBES TO DETERMINE THE ELECTRON DENSITY SURROUNDING RE-ENTRY VEHICLES

By: W. E. SCHAREMAN

Prepared for:

NATIONAL AERONAUTICS AND SPACE ADMINISTRATION
LANGLEY RESEARCH CENTER
LANGLEY STATION
HAMPTON, VIRGINIA 23365

CONTRACT NAS1-3942

STANFORD RESEARCH INSTITUTE

MENLO PARK, CALIFORNIA

*SRI

STANFORD RESEARCH INSTITUTE
MENLO PARK, CALIFORNIA

June 1965

Final Report

THE USE OF LANGMUIR PROBES TO DETERMINE THE ELECTRON DENSITY SURROUNDING RE-ENTRY VEHICLES

Prepared for:

NATIONAL AERONAUTICS AND SPACE ADMINISTRATION
LANGLEY RESEARCH CENTER
LANGLEY STATION
HAMPTON, VIRGINIA 23365

CONTRACT NAS1-3942

By: W. E. SCHARFMAN

SRI Project 5034

Approved: T. MORITA, MANAGER
ELECTROMAGNETIC SCIENCES LABORATORY

D. R. SCHEUCH, EXECUTIVE DIRECTOR
ELECTRONICS AND RADIO SCIENCES

Copy No. 78

ABSTRACT

Langmuir probes can be extremely useful tools for re-entry physics studies. However, classical probe theory, as developed by Langmuir, is predicated upon a number of conditions that will not hold true over an entire trajectory. It is necessary to determine the errors involved in the inferred plasma parameters and to develop a theory that will enable one to interpret the data over the complete trajectory. 27529

In this report classical probe theory is reviewed, and the conditions under which it is applicable are pointed out. Some later developments in probe theory that account for flow velocity in the free-molecular case are also discussed. The use of flush probes on re-entry vehicles is considered, both theoretically and experimentally.

The theory of ion collection using long cylinders in a supersonic flow, where the probe radius is of the order of the mean free path, has been confirmed over a range of electron densities by a series of measurements in an arc-driven shock tube. Probe data were checked with equilibrium calculations and with a 33-Gc microwave interferometer. Agreement was better than a factor of two among the three means of determining electron density.

Evidence is given for a scaling relation for cylindrical probes in continuum flow. The product $n_+ r_p$ (where n_+ is ion density and r_p is probe radius) is a constant with initial pressure and probe radius, and depends only on shock velocity.

Preliminary results for a narrow wedge probe at zero-degrees angle of attack indicate that this geometry may be practical for the design of a probe for use on re-entry vehicles.

Preliminary measurements have also been made with flush probes mounted in the walls of the shock tube. The measured results are interpreted using a simple boundary-layer theory for the electron concentration near the wall. Good qualitative and fair quantitative agreement have been obtained.

ACKNOWLEDGMENT

It is a pleasure to acknowledge the many stimulating discussions with H. Bredfeldt and H. Guthart of this laboratory. The measurements were capably performed by J. Granville.

CONTENTS

ILLUSTRATIONS

TABLES

I INTRODUCTION

The determination of the electron density surrounding a re-entry vehicle from gas-dynamic calculations is hampered by uncertainties in the rate constants of the ionization processes as well as by the effects of ablation products. However, calculations have been made, and it would be desirable to be able to check them with flight-test data.

One common method of determining electron density is to measure the absorption and phase shift of microwaves that propagate through the plasma sheath. However, these measurements give only limited information; one obtains only an integrated value of absorption and phase shift. In order to interpret the results in terms of electron density and collision frequency, it is necessary to estimate the spatial distributions of these parameters, although the spatial distribution is itself one of the parameters of interest. In addition, the dynamic range of parameters that can be measured by such methods in a realistic flight test is usually quite small. For a given microwave frequency, it is usually possible to determine the electron density only when the plasma frequency is of the order of the microwave frequency.

The limitations in the use of microwaves apply equally well to the technique in which the reflected signal is monitored. This signal is appreciable only when the plasma frequency is greater than the microwave frequency. When the plasma frequency is greater than the microwave frequency the reflected signal approaches a constant value, and no further information about the plasma is obtained. Therefore, the reflected signal technique is useful mainly in determining when the plasma frequency is the same as the microwave frequency and is noted by the rapid rise in reflected signal.

As interest in hypersonic flows of the order of Mach 30 increases, the usefulness of microwaves becomes even smaller. This is true because the electron densities produced at these velocities are so high that it would be impracticable to fly transmitters of sufficiently high frequency

to prevent the plasma frequency from being higher than the microwave frequency, once ionization starts.

An alternative technique for measuring electron density during flight tests is to use electrostatic probes. We shall adopt the convention of calling electrostatic probes that operate under the classical Langmuir conditions "Langmuir" probes. All probes that do not satisfy these conditions will be called simply "electrostatic" probes. It is possible to design these probes so that measurements can be made with a spatial resolution of less than 1 mm. Thus, use of a probe that could move radially outward from the re-entry vehicle would make it possible to determine the spatial distribution of electrons. Alternatively, one could use several probes mounted at different radial distances from the vehicle surface.

Langmuir probes are inherently capable of measuring a wide range of electron densities. They appear to be worthy of consideration for flight tests. Probe theory, however, is predicated upon a number of conditions that will not hold true over an entire trajectory. It is necessary to determine the errors involved in the inferred plasma parameters and to develop a theory that will enable one to interpret the data over the complete trajectory.

The theory of Langmuir probes is well established for the free-molecular case, i.e., when the mean free path is much greater than the probe radius and the sheath thickness.[1] Furthermore, the classical Langmuir theory does not consider the case of a flowing plasma moving with supersonic velocity. For probes to be useful as diagnostic tools aboard re-entry vehicles it is necessary to have a theory that will include flow effects. The usefulness of such probes will be further enhanced if measured probe current under short mean free path conditions can be interpreted to yield values for the electron density.

On a previous contract (NAS1-2967) we used rapidly sweeping voltage circuitry to obtain complete current voltage characteristics for equal-area probes in an electromagnetic shock tube. These probes indicated electron densities that checked microwave measurements even when the

probe radius was of the order of the estimated mean free path. However, the actual value of the mean free path was quite uncertain.

Under this contract we are studying both the effects of flow velocity and short mean free path. We have used an arc-driven shock tube to produce equilibrium, supersonic samples of partially ionized air. The properties of the gas, including mean free path, are thus well known. By inserting a series of cylindrical probes of varying diameter into this flow we have obtained several interesting results. Theories of probe operation have been recently developed for the case of free-molecular supersonic flow, and our data show that these theories can be used to measure electron density for probe diameters up to several mean free paths. A quantity of data was also gathered for the case that is more difficult to handle theoretically--supersonic flow with the mean free path much smaller than the probe diameter. It is to be expected that under these conditions the probe will have a shock surrounding it, and thus interpretation of the probe current in terms of the incident plasma properties would have to take into account the change in properties due to the shock. The problem is further complicated by the fact that the flow times around the probe are so short that for a large range of conditions the flow around the probe will not be in equilibrium. It would thus be necessary to introduce the appropriate rate constants and solve the flow problem with finite time chemistry. This is a very difficult problem theoretically, and it is clear that solutions would not be any more accurate than the rather poorly known rate constants.

Our approach has been first to gather data on probe operation under these conditions and then to see whether there are any applicable scaling relations which enable one to generalize the results. Such scaling relations could also be used by the theoretician as a guide in identifying the dominant processes and hence simplifying his analysis. Through analysis of the data we have gathered to date, it appears that a scaling relation does exist when the probes are in the continuum flow regime. We cautiously use the word "appears" because the data are too scanty for us to be sure that the scaling extends over the full continuum flow regime.

II ELECTROSTATIC PROBE THEORY

In this section we summarize some of the results of classical Langmuir theory and point out its limitations. Next, we discuss recent work on the operation of electrostatic probes in supersonic and hypersonic flowing plasmas under free-molecular conditions. Two geometries are considered: right circular cylinders and small-angle wedges. A qualitative discussion of probes operating in the continuum flow regime is given. Finally, the operation of flush probes is considered. The work on flush probes was supported by the Advanced Research Projects Agency under Contract SD-103, and is included here because it is of interest in connection with possible probe configurations for re-entry vehicles.

A. OPERATION OF PROBES--CLASSICAL THEORY

An electrode or probe inserted into a plasma will collect charges until it has sufficiently high potential with respect to the plasma to neutralize the net charge arriving at the electrode, i.e., the electrode potential is such as to equalize the electron and ion flux. If the electrode potential is made increasingly negative with respect to a second electrode, fewer and fewer electrons will reach the probe until only positive ions are collected. Conversely, if the probe potential is made increasingly positive with respect to the second electrode (and the area of the second electrode is greater than that of the first by the square root of the mass ratio of ions to electrons), the probe will collect only electrons.

When electrostatic probes are used to collect electrons, the saturated electron current density, J_-, is related to the electron density, n_-, by the expression

$$J_- = \frac{n_- e v_-}{4}$$

where

v_- is the electron random velocity = $\sqrt{\frac{8kT_-}{\pi m_-}}$

e is the electron charge

k is Boltzmann's constant

T_- is the electron temperature

m_- is the electron mass.

When ions are collected, the relationship between ion current density and ion density (or electron density, assuming that $n_- = n_+$) has been shown by Bohm et al.[2] to be approximately

$$J_+ = 0.4 n_+ e v_+ \quad , \tag{1}$$

where

v_+ is the velocity with which ions reach the sheath = $\left(\frac{2kT_-}{m_+}\right)^{\frac{1}{2}}$

m_+ is the ion mass.

From the expression for saturated ion current density, it can be seen that if the ion mass and electron temperature are known or can be estimated, a measurement of the ion current density is sufficient to determine the electron density. Estimates can often be made of ion species, and hence ion mass; in addition, the electron temperature also may be estimated from gas-dynamic considerations. In either case, errors in these quantities will not be very serious, since they both enter into the expression for current density as the square root. For example, if the temperature at a certain region on a re-entry vehicle is estimated at 3000°K when it is really only 2500°K, the error in ion density is only about 10 percent.

Between these two saturated regions is a region that may be used to determine the electron temperature.

For potentials below plasma potential, the electrons see a potential barrier that only the higher-energy electrons can overcome to be

collected at the electrode. If, at the sheath edge, the random electron current density is J_-, then at a point in the sheath where the potential is V volts below the plasma potential, the electron current density is $J_- \exp(- eV/kT_-)$.

The net current density is the algebraic sum of the ion and electron current densities, so that the net current density is

$$J_{net} = J_- \exp(- eV/kT_-) - J_+ \quad . \tag{2}$$

Bringing the ion current density to the left side of the equation and taking logarithms of both sides, we obtain

$$\ln(J_+ + J_{net}) = \ln J_- - eV/kT_- \quad . \tag{3}$$

Thus T_- may be found from a semilogarithmic plot of $J_+ + J_{net}$ as a function of V. This plot will be a straight line with slope e/kT_- for a Maxwellian energy distribution.

Since we have found that measurements on the ion-saturation-current side are more accurate than measurements on the electron-saturation-current side, we shall restrict the following discussion to the ion side.

In making probe measurements, one measures current rather than current density. Therefore, it is necessary to know the relation between these two quantities. From a consideration of the formation of plasma sheaths, the sheath thickness, d_s, can be approximated by

$$d_s = \lambda_D \eta^{\frac{3}{4}} \tag{4}$$

where

$$\lambda_D = \text{Debye length} = \sqrt{\frac{\epsilon_0 kT_-}{n_- e^2}} = 7\sqrt{\frac{T_-}{n_-}} \text{ cm}$$

$$\eta = \left|\frac{eV}{kT_-}\right|$$

and ϵ_0 is the permittivity of free space. Equation (4) is the expression for the sheath thickness for space-charge-limited flow in a planar geometry. This equation is obtained by equating the current density given by the planar space charge equation to the random current density of Eq. (1). The approximation of a planar solution for sheath thickness is applicable to nonplanar probes only when the sheath thickness is small compared to the probe radius. When the sheath thickness is large, it can be shown[1] that the current collected by a probe may be made independent of the sheath dimensions, so that the approximation of Eq. (4) is no longer required.

The overall sheath radius, a, is given by

$$a = r_p + d_s \quad , \tag{5}$$

where r_p is the probe radius. If the probe radius is larger than the sheath thickness, then all the particles that pass through the sheath edge will be collected by the probe and the probe area will be approximately equal to the sheath area. Under these conditions, the probe current for a cylindrical probe is

$$I_+ = 2\pi r_p L J_+ \tag{6}$$

and for a spherical probe,

$$I_+ = 4\pi r_p^2 J_+ \quad , \tag{7}$$

where

I_+ is the probe current

L is the probe length.

A further consequence of requiring the probe sheath to be of the same order as the probe radius is that the probe current will be relatively insensitive to the probe potential, as long as the potential is sufficiently negative to draw saturation current. This is so because

the increase in probe current with potential is due to an increase in the sheath thickness, which increases the area through which current passes. However, since the sheath area is approximately equal to the probe area, there will be no significant change in the current-collecting area.

In order to ensure this condition, it is necessary that

$$r_p \gg d_s$$

and that the probe potential be such that

$$\eta = \left|\frac{eV}{kT_-}\right| \gg 1 \quad .$$

If these conditions are not satisfied, the current will be a function of voltage and will no longer be simply equal to the product of the random current density and the physical area. Interpretation of probe current in terms of electron densities under these conditions becomes more complicated, but verified theories for such interpretations are available.[3-6] The results are summarized in the following.

When $\eta \gg a/r_p$, where a is the sheath radius and r_p is the probe radius, the current is a function of a/r_p:

$$I_+ = (a/r_p)2\pi r_p L J_+ \qquad \text{(for a cylindrical probe)}$$

and

$$I_+ = (a/r_p)^2 4\pi r_p^2 J_+ \qquad \text{(for a spherical probe)} \quad .$$

When $\eta \ll a/r_p$ and $\eta > 2$, the current is a function of potential but is independent of a/r_p.

$$I_+ = \frac{2}{\sqrt{\pi}} \sqrt{\eta + 1}\ 2\pi r_p L J_+ \qquad \text{(for a cylindrical probe)}$$

and

$$I_+ = \eta 4\pi r_p^2 J_+ \qquad \text{(for a spherical probe)} \quad .$$

These are asymptotic cases. Hok[4] has calculated the dependence of ion current on ion density and temperature for a cylindrical probe for the whole range of η and a/r_p. For the spherical probe, the intermediate range of η and a/r_p can be approximated using the solution of Allen et al.[5]

Hok's results are shown in Fig. 1, where Hok has plotted the current, normalized to the product of the physical area and the random current density, as a function of η for a wide range of values of the ratio of the sheath to the probe radius. The asymptotic solutions given above are illustrated in this figure. When $a/r_p \approx 1$, the normalized current is 1; when $a/r_p < \sqrt{\eta}$, the curves flatten, and the normalized current is independent of η and equal to a/r_p; when $a/r_p > \sqrt{\eta}$, the normalized current is equal to $\frac{2}{\sqrt{\pi}} \sqrt{\eta + 1}$ and independent of a/r_p.

Although this plot is extremely useful for a general understanding of the different regimes under which a probe may operate, we must know a/r_p in order to use it for determining the electron density from a measurement of current. The space-charge-limited diode equation may be manipulated so that values of a/r_p can be found in terms of the measured current and other measurable parameters--probe length, diameter, and potential. The results are shown in Fig. 2. The probe-to-plasma potential, V, is not the same as the applied potential, but can be taken as the applied potential plus 5 kT/e for purposes of estimating a/r_p. In order to estimate η, it is necessary to have some idea of the temperature, but for large values of η, this term, which only varies as the square root, does not contribute significantly.

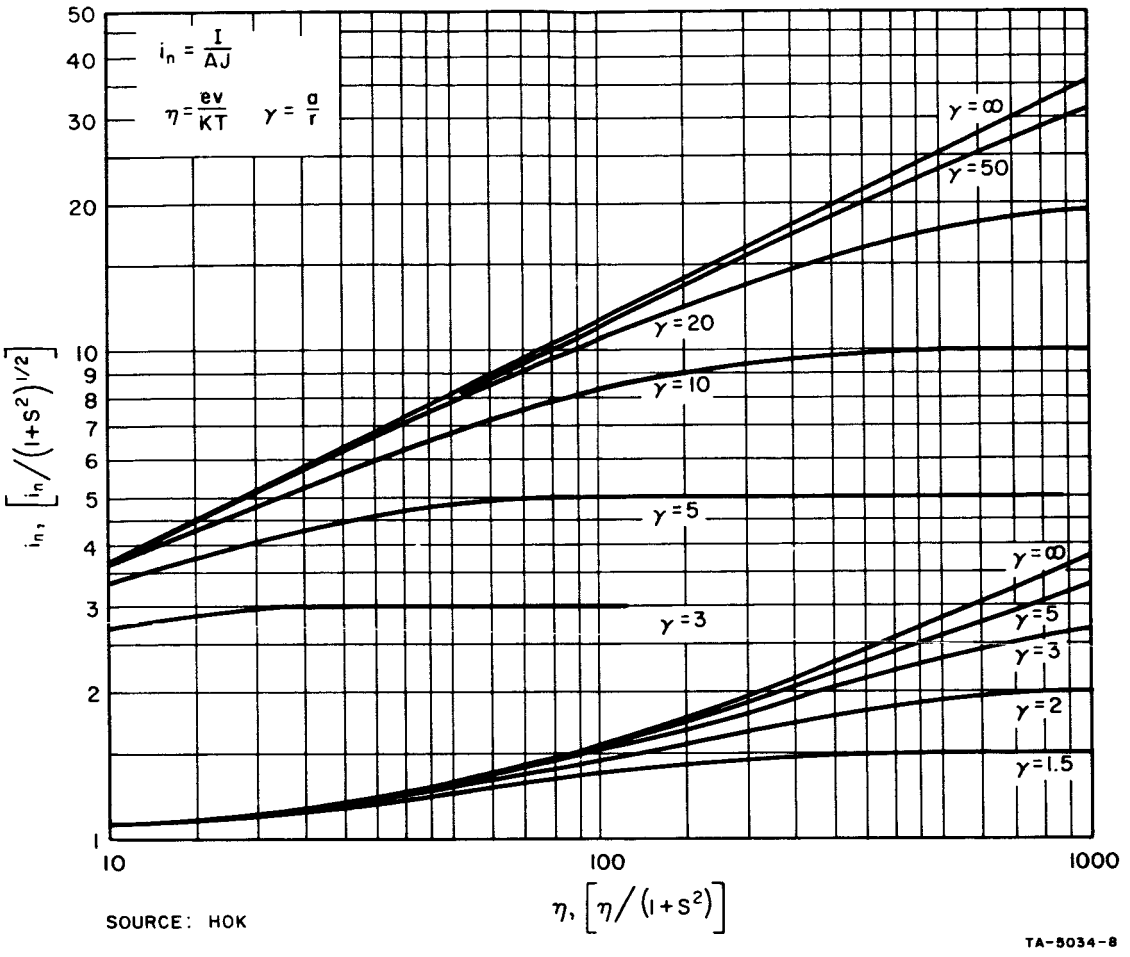

FIG. 1 NORMALIZED PROBE CURRENT AS A FUNCTION OF η, WITH a/r_p AS A PARAMETER

Figures 1 and 2 combined enable one to transform the measured current into electron density (if the temperature is known) without the necessity of considering which asymptotic solution is applicable.

B. CONDITIONS FOR APPLICABILITY OF CLASSICAL PROBE THEORY

There are a number of conditions that must apply for classical probe theory to be applicable:

(1) The mean-free path must be much larger than the probe dimension. This is necessary to ensure that the probe does not disturb the plasma, and may be

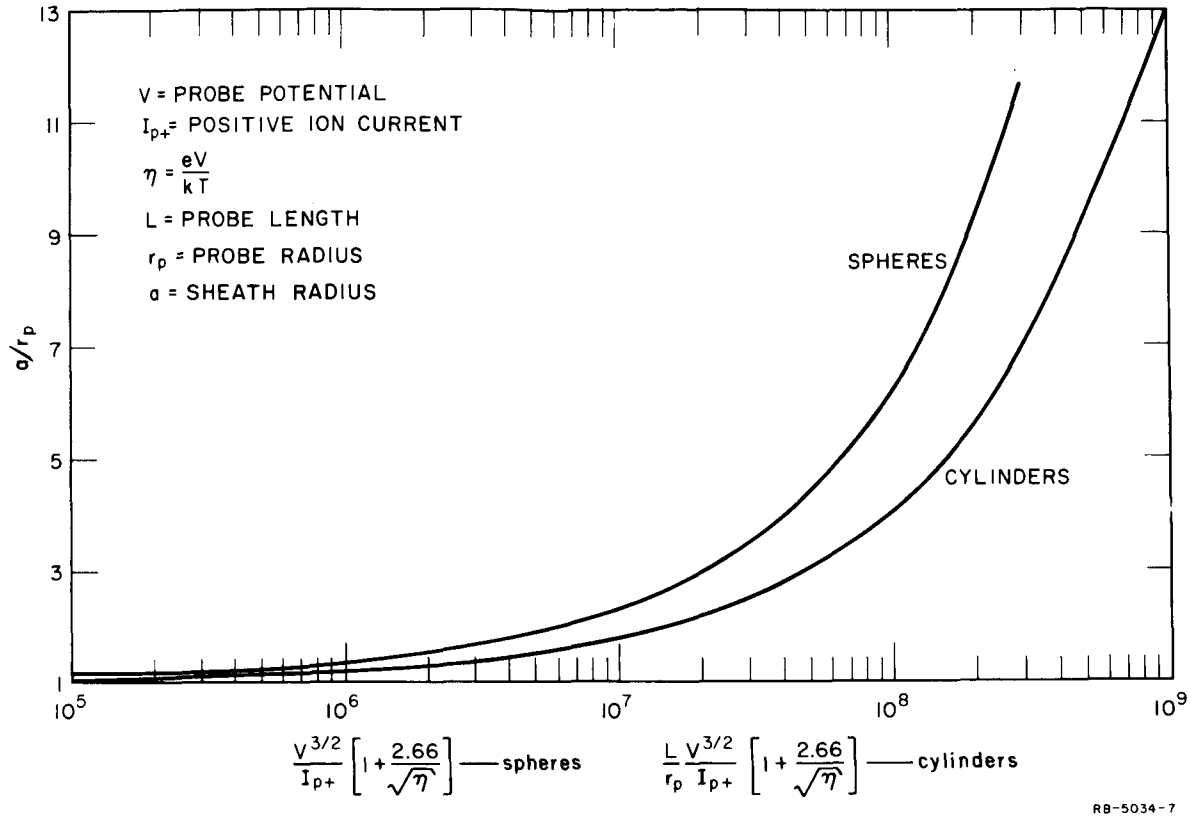

FIG. 2 a/r_p AS A FUNCTION OF THE MEASURED PARAMETERS

written as

$$r_p < \lambda \ (\lambda = \text{mean-free path}) \quad .$$

(2) The sheath thickness must be much less than a mean free path. This ensures that there are no collisions in the sheath, an assumption used in deriving the relations between current and probe potential. This may be written as

$$d_s = a - r_p < \lambda \quad .$$

(3) There is no net flow velocity. This may be written as

$$v_f = 0 \quad .$$

(4) There is frozen flow across the sheath; i.e., there is no ionization or ionization loss--such as recombination--in the sheath. This may be expressed as a current-continuity relation

$$\nabla \cdot J = 0 \quad .$$

(5) So far we have concentrated on the current collection properties at only one electrode; however, for current flow there must be another electrode in contact with the plasma to complete the circuit. This second electrode must have sufficient area for current collection so that the sheath around it does not limit current flow in the system. This consideration of area is especially important in making the temperature measurement and in ensuring that conditions are proper for measuring the random electron current density. If the area is too small, a saturation current will exist for both ion and electron currents; however, the electron saturation current will be less than the full random electron current density. The area ratio is related to the ratio of mobility of electrons and ions; in air, the ratio must be at least 250.

$$\frac{\text{Area Electrode 1}}{\text{Area Electrode 2}} > 250 \quad .$$

If the electrode-area ratio is less than this value, the full random electron current density will not be measured at any potential. The electron temperature can be inferred from the current/voltage plot, but the interpretation will be somewhat different than that outlined above. The theory of probe operations at area ratios less than that indicated above has been worked out by Johnson and Malter.[6]

C. ION COLLECTION WITH FLOW VELOCITY--FREE-MOLECULAR CASE

Several theoretical treatments[7-9] of the problem of ion collection in a flowing plasma have been made for the case where there are no collisions in the sheath and where the probe is smaller than the mean free path. It is also usually assumed that the form of the sheath is not disturbed by the flow.

The theoretical relation between probe current and flow velocity is shown in Fig. 3 for the case where the sheath thickness is small compared to probe radius. Under these conditions, a useful parameter that indicates whether the flow has a significant effect on ion current collection is the ratio of flow velocity, v_f, to thermal velocity, $v_+ [v_+ = (2kT_-/m_+)^{\frac{1}{2}}]$. This ratio is approximately 0.8 times the Mach number for air before dissociation. When the Mach number is much less than unity, the effect of flow is negligible. When the Mach number is greater than about three, the current is essentially made up of the flow of ions into the projected area of the probe. Thus, for $a/r_p \approx 1$,

$$I_+ = n_+ e v_f 2 r_p L \qquad \text{(for cylindrical probes with flow perpendicular to axis)}$$

and

$$I_+ = n_+ e v_f \pi r_p^2 \qquad \text{(for spherical probes)} \quad .$$

When the sheath thickness is larger than the probe radius, the problem is more complicated. In addition to the Mach number, one must consider the relation between the potential field around the probe, which pulls the ions toward the probe, and the inertia of the ions, which can carry them through the potential field without their being collected. This problem was treated by Smetana;[9] his results are shown in Fig. 4. The actual current collected is obtained by multiplying the random current collected through the physical area of the probe by the factor F, given in Fig. 4.

When S (which is v_f/v_+) is equal to zero, we have the case discussed previously, when $\eta \ll a/r_p$; i.e., the current increases with

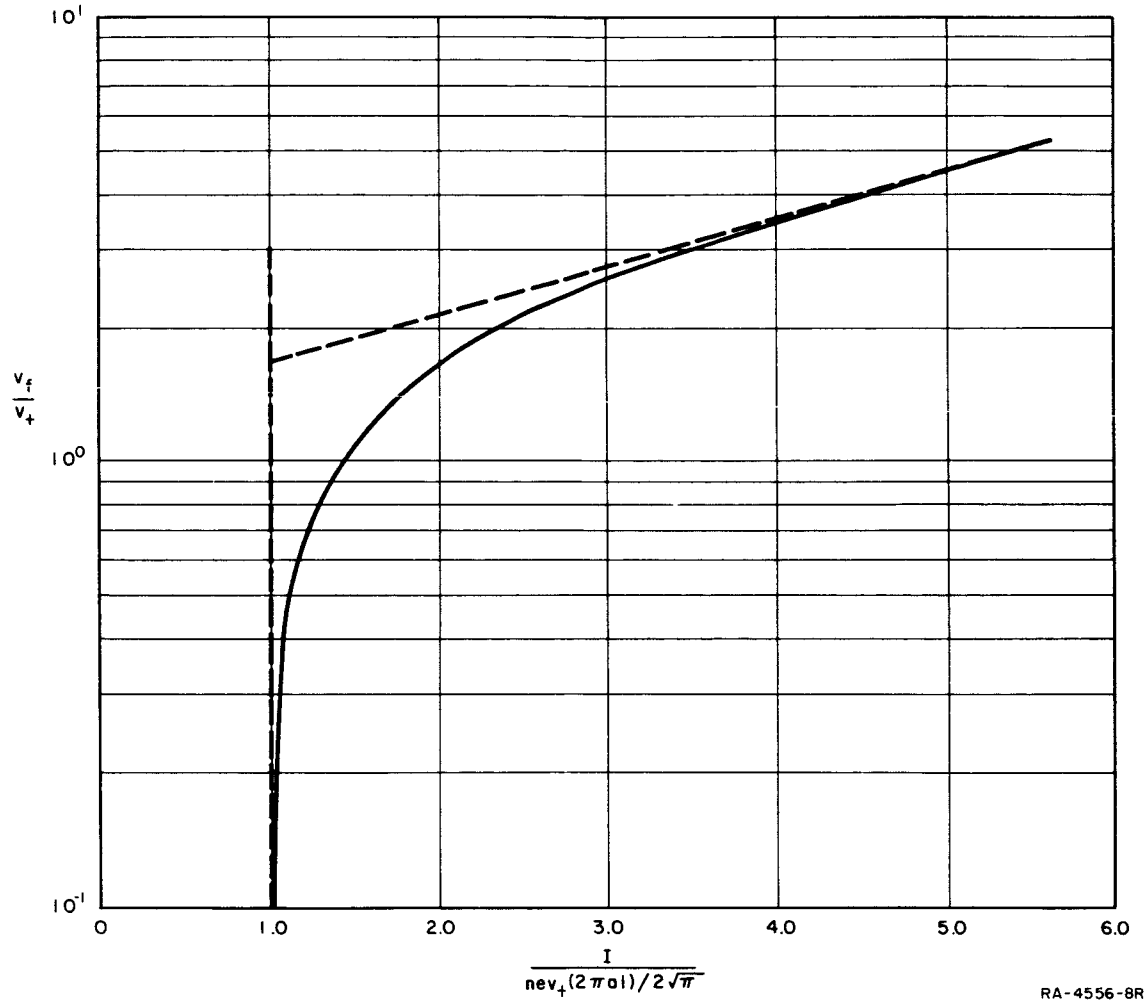

FIG. 3 RATIO OF DIRECTED TO RANDOM VELOCITY AS A FUNCTION OF THE NORMALIZED CURRENT COLLECTED BY A PROBE PERPENDICULAR TO THE DIRECTED VELOCITY

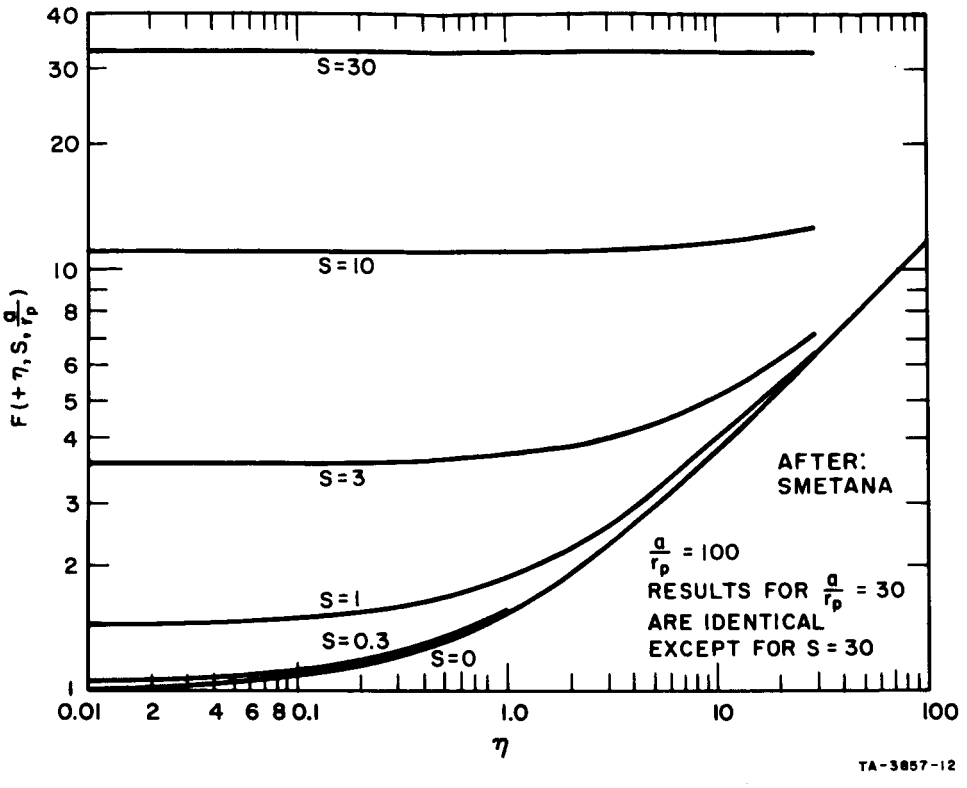

FIG. 4 NONDIMENSIONAL FLUX DENSITY OF ATTRACTED PARTICLES AS A FUNCTION OF DIMENSIONLESS PROBE POTENTIAL FOR VARIOUS SPEED RATIOS, S, AT $a/r_p = 100$

$(\eta + 1)^{\frac{1}{2}}$. As S becomes greater than zero, the current at low values of η increases; at high values of η, the current is unchanged.

This behavior can be explained as follows. At low η and large a/r_p, the potential field is so weak that most of the ions that enter the sheath orbit past the probe and leave the sheath without being collected. Under these conditions, the current collected is equal to the random current density times the physical area of the probe. Thus, at low η, when the current is only proportional to the physical area of the probe with S = 0, the addition of flow increases the current collected, just as it would in the case of $a/r_p \approx 1$. When values of S are large, $F \approx S$ and $I_+ \approx nev_f A_p$, where A_p is the projected area.

At higher values of η, with S = 0, a larger percentage of the ions that enter the sheath are collected by the probe. From simple orbital calculations one finds that for a given potential V and particles

entering with initial energy V_0, the radius at which particles will just be collected is $r_a = r_p(1 + V/V_0)^{\frac{1}{2}}$. Therefore, the current that is collected is proportional to the flux entering the sheath out to a radius r_a times the area at that radius:

$$I_+ \propto nV_0^{\frac{1}{2}} \times r_p(1 + V/V_0)^{\frac{1}{2}} \quad .$$

For S equal to zero, $V_0 = kT_-/e$ and I_+ is given by the equation for $a/r_p > \eta$. In the limit of $\eta \gg 1$, $I_+ \propto V^{\frac{1}{2}} r_p$. When $S > 0$, the flux is proportional to $SV_0^{\frac{1}{2}}$ and $r_a = r_p(1 + V/S^2V_0)^{\frac{1}{2}}$. Thus, the absorption radius is decreased, while the flux entering the sheath increases so that

$$I_+ \propto nSV_0^{\frac{1}{2}} \times r_p(1 + V/S^2V_0)^{\frac{1}{2}} \quad .$$

When $\eta \gg S^2$, this reduces to the same value as when $S = 0$.

With this understanding of current collection under flow conditions, let us reconsider Fig. 1. Using the asymptotic solutions for $S = 0$ and $S \gg 1$, we can formulate a transformation of the coordinates which will be useful for analyzing probes in flowing as well as non-flowing plasmas.

The abscissa, η, is the ratio of the potential energy of the electric field to the kinetic energy of the electrons. For a flowing plasma, the kinetic energy of the electron, at large values of S, is S^2 times as great as their kinetic energy of random motion. Thus, if we replace η by η/S^2, the abscissa will measure the same ratio of energies, including that of the flowing plasma. A more correct formulation would be $\eta/(1 + S^2)$, since we know that when $S = 0$, the transformation should reduce to η.

Similarly, the ordinate, I/AJ, is a measure of the ratio of the current collected by the probe to the random flux which enters the physical area at a velocity proportional to the square root of the kinetic energy. But with flow, the flux is increased by a factor S, and therefore the ordinate may be written as I/(AJ)S, or, to cover the case of S = 0, $I/(1 + S^2)^{\frac{1}{2}}(AJ)$.

If the ordinate and abscissa in Fig. 1 are transformed in this way, we obtain a chart for probe operation both with and without flow and for both large and small sheaths. The values obtained in this way agree with Smetana's[9] results quite well. On the other hand, there is very little experimental verification of these theoretical treatments. In the experimental section of this report we shall present evidence for the case of small sheaths.

D. CYLINDRICAL PROBES IN CONTINUUM FLOW

When the probe dimension becomes much larger than the mean free path, it is to be expected that a shock will be formed around the probe.[10] No theoretical treatment exists for cylindrical probe operation under such conditions; in this section we merely mention some of the processes that might be operative.

When a shock forms around a cylindrical probe in a flowing plasma, the probe will be "isolated" from the incident plasma in the sense that it will be sampling conditions behind the secondary shock rather than conditions in the incident plasma. The probe will still measure the flux across the sheath, but the problem will be in relating this flux to the incident quantities.

The gas which goes through the shock will be compressed, so that even if no additional ionization occurs, the electron density will increase from that of the incident flow. The gas velocity will be slowed down and its direction changed. Since the gas temperature will increase, the Mach number behind the shock will be reduced.

The shock detachment distance is essentially a function of probe radius and Mach number, being roughly of the order of a few tenths of

the probe radius. If this distance is too short for chemical relaxation to occur, the gas will be in a condition of nonequilibrium. The gas molecules may flow around the probe before their high translational energy can be converted into ionization and dissociation.

Even if the gas does equilibrate, a boundary layer will always form and will almost certainly not be in ionization equilibrium. (The electron density will not equal the value for equilibrium conditions at a given temperature and gas density.) Except for very weak shocks, the sheath will generally be embedded in the boundary layer, so that it is important to be able to relate the boundary-layer parameters to the incident flow parameters. Recombination in the boundary layer may be important at the very high electron densities formed by the secondary shock.

Adequate handling of this case theoretically would be a formidable undertaking. Our approach has been first to gather data on probe operation under these conditions, and then to see whether there are any applicable scaling relations which enable one to generalize the results. Such scaling relations could also be used by the theoretician as a guide in identifying the dominant processes and simplifying his analysis. The results of such an experimental program will be presented in Sec. III.

E. NARROW WEDGE PROBES

Use of a wedge structure is of interest because the wedge offers the possibility of providing minimal disturbance of the flow field near the probe while maintaining adequate mechanical strength. To avoid disturbing the flow, cylindrical probes must have radii that are small compared to the mean free path, and thus they are mechanically poor. With a wedge, it may be possible to maintain the flow undisturbed simply by the geometry of the structure, and since the base of such a wedge would be much larger than a free-molecular cylinder, the wedge would be much stronger.

Recent theoretical investigations of the flow field about slender cones under re-entry conditions have indicated that these bodies produce

electrons only in the boundary layer surrounding the body.[11,12] Furthermore, the values of the electron densities in the boundary layer are quite low compared to the electron densities produced by blunt-nosed bodies at the same altitude and velocity as the cones. On slender cones the boundary-layer electrons are produced only after the gas has moved many feet down the body.

Applying these ideas to probes, we thought it would be interesting to construct a two-dimensional wedge in order to determine whether the shock structure produced by such a body would minimize the change of the incident flow parameters. There are two ways in which such a wedge could be used to advantage. First, if the leading edge of the wedge were made sufficiently sharp so that it was free-molecular, this edge could be electrically isolated from the rest of the wedge and used as a free-molecular electrode. The changes in electron density due to the shock formed around the wedge would not affect the plasma at the electrode, because in supersonic flow, changes produced downstream from a point cannot propagate upstream and alter the gas properties at the upstream point. Thus, changes produced by the shock structure downstream of the leading edge of the wedge could not reach the leading edge. An example of such a probe is a small wire used as the leading edge of a wedge made of dielectric. The wire serves as the electrode, and the rest of the wedge is a mechanical support.

Alternatively, the entire wedge could be used as an electrode. In this case, the shock structure produced by the wedge would be sufficiently weak and the flow times sufficiently short that the incident plasma would not be appreciably changed in the vicinity of the probe.

In order to interpret the current collected by a narrow wedge, we have used a free-molecular theory derived for a flat plate inclined at an angle to the flow. The results are shown in Fig. 5.[8] This figure shows a velocity factor which must be used to multiply a constant factor in order to give the net current

$$I = \frac{n_+ e\, v_+}{4} \text{ (velocity factor) (area)} \quad .$$

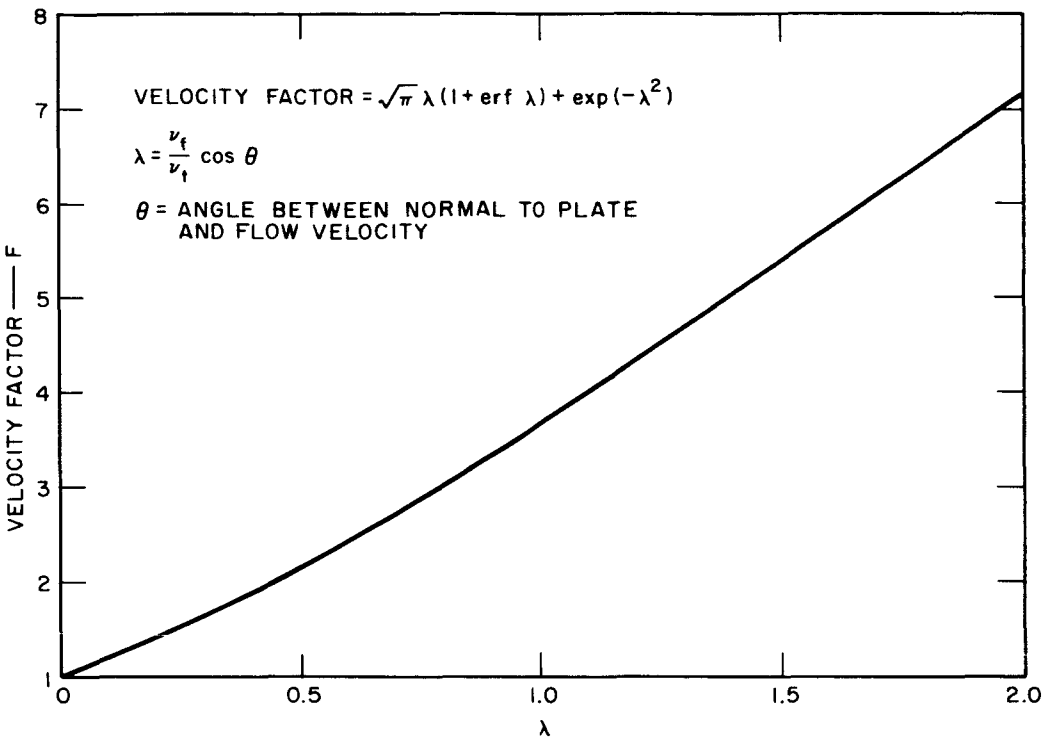

SOURCE: HOEGY & BRACE, U. of Michigan, Scientific Report JS-1, September 1961

TA-5034-2

FIG. 5 VELOCITY FACTOR AS A FUNCTION OF VELOCITY PARAMETER FOR FLAT PLATES

Note in Fig. 5 that the velocity factor tends to 1 as the angle between the flow velocity and the normal to the plate increases. Under these conditions, the flow velocity becomes less important, because the area projected into the flow tends toward zero as θ goes to 90 degrees. When this occurs, the current collected is attributable only to the thermal motion of the electrons.

A narrow wedge at zero-degree angle of attack can be considered as two flat plates inclined at opposite angles to the flow. Thus, we can interpret the current to the wedge using Hoegy's and Brace's theory.[8] Of course, their theory is for free-molecular conditions, whereas we are interested in continuum flow conditions. However, if the wedge does not disturb the flow, the free-molecular theory may be applicable even under continuum conditions. The results of measurements with a narrow

wedge of about 40 mean free paths at the base is presented in Sec. III-B, "Experimental Results."

F. ION COLLECTION BY FLUSH PROBES IN NONUNIFORM PLASMAS*

In order to avoid perturbations of the flowing plasma surrounding a re-entry vehicle, it may be necessary to place probes on the surface of the vehicle rather than in the flow field. Since the electron density varies as a function of distance from the vehicle surface, the question arises as to what current the probe will measure.

Ordinarily, a probe samples the plasma at the edge of the sheath. For the classical case, where the mean free path is much larger than the sheath radius, the density without the probe present cannot change significantly in a sheath thickness. However, in the immediate vicinity of the vehicle surface, the electron density may be so low that the sheath extends out many mean free paths to a point where the electron density has increased significantly. Under these conditions, there will be many collisions in the sheath. The following is a first attempt at a one-dimensional theory to handle this case.

A planar geometry is assumed, with the probe sufficiently large that the physical and sheath areas are approximately equal; most of the current drifts into the sheath from a plane d_s centimeters from the surface. Assuming that there is neither recombination nor ionization in the sheath, an equation for the current may be written as:

$$I = An_{+s}ev_{+}/4 \tag{8}$$

where

n_{+s} = ion density at the sheath edge

v_{+} = thermal velocity at the sheath edge.

---

*Work accomplished under ARPA Contract SD-103, Order 281-62.

If these assumptions are correct, a measurement of the ion current coupled with a knowledge (either theoretical or from another measurement) of the thermal velocity at the sheath edge is sufficient to determine the ion density at the sheath edge. In order to establish the location of the sheath edge, it is assumed that the charge density redistributes itself within the sheath in such a manner that the current flowing across the sheath to the electrode is governed by the same relationships as for a space-charge-limited diode at high pressures.[13] This relationship is given by

$$I = 9/8\epsilon_0\mu_+ \frac{V^2}{d_s^3} A \qquad (9)$$

where

μ_+ = ion mobility

V = potential across the sheath

d_s = distance from the wall to the sheath edge

A = area of the electrode.

Equation (9) may be solved for d_s in terms of the experimental parameters, I, V, and μ_+. Equation (9) is for a constant mobility through the diode. For a sheath formed near the vehicle surface, the mobility will vary through the sheath, decreasing toward the surface by a factor that is generally less than three. The diode equations have been solved with a mobility decreasing exponentially from the cathode. It is found that for a decrease in mobility of a factor of three, the solution has the same form as Eq. (8) with μ_+ equal to the mobility at the sheath edge, but with the constant reduced to about three quarters of the value shown above. Considering the order of the other approximations, Eq. (8) will be used as it stands, with μ_+ equal to the mobility at the sheath edge.

If these assumptions are valid, the measurement of current in an electrode flush with the vehicle surface will enable one to determine the ion flux at a distance d_s from the surface. It is interesting to

note from Eq. (9) that the sheath edge may be moved by varying the probe potential, so that there is the possibility of measuring the electron density profile near the wall. The distance d_s will be a function of the plasma parameters as well as the potential. For reasonable potentials, d_s will be of the order of 0.025 mm (1 mil) for electron densities around 10^{13} electron/cc, and will increase to about a centimeter for densities around 10^7 electron/cc. Thus, the degree to which the boundary layer near the vehicle can be sampled by a flush probe will depend strongly upon the density levels involved.

Preliminary results using this theory to interpret data taken in a shock tube are discussed in Sec. III.

III ELECTROSTATIC PROBE MEASUREMENTS

A. INTRODUCTION

In order to check the theory of probe operation in supersonic ionized flows under free-molecular conditions and to gather data for construction of a theory under continuum flow conditions, measurements were made in a pressure-driven shock tube. The characteristics of the shock tube are described in the appendix.

A set of three cylindrical probes was used for the measurements. The probe dimensions were 0.01 inch (diameter) × 1/4 inch (length); 1/16 × 5/8 inch; and 1/4 × 2-1/2 inch. Each probe was at least twenty times longer than its radius so that end effects would be negligible.

Measurements were made at two initial shock-tube pressures, p_1 = 1 mmHg and p_1 = 0.1 mmHg. Shock velocities ranged from about 3 to 5 mm/μsec at the higher pressure, and from 4 to 7 mm/μsec at the lower pressure. The ratio of shock velocity to v_+, behind the shock, varied from about 2.3 to 3.7 over this range of pressures and shock velocities.

The probe sizes, in units of neutral-neutral mean free paths behind the incident shock, are shown in Table I. For strict free-molecular flow the probe radius should be smaller than the incident mean free path. This was not the case for any of the above conditions, but, as will be discussed later, the 0.01- × 1/4-inch probe at p_1 = 0.1 mmHg operated as though it were in the free molecular regime. There is no sharply defined value of r_p/λ above which the flow can be considered a continuum, but from the work of Probstein a ratio of about $r_p/\lambda = 30$ seems sufficient for transition well into the continuum regime.[10] If this is true, then only the 1/4-inch diameter probe at 0.1 mmHg and the 1/16- and 1/4-inch probes at 1 mmHg were in continuum flow. Certain scaling relations that were discovered upon analyzing the data reinforce the idea that these probes were operating in a similar flow regime.

Table I

EXPERIMENTAL PROBE SIZES

p_1 = 0.1 mmHg

v (mm/μsec)	Mean Free Path λ_2 (mils)	r_p/λ_2		
		r_p = 5 mils	r_p = 31 mils	r_p = 125 mils
4	2.0	2.5	15	62
5	1.85	2.7	17	68
6	1.57	3.2	20	80
7	1.38	3.6	22	91

p_1 = 1 mmHg

v (mm/μsec)	Mean Free Path λ_2 (mils)	r_p/λ_2		
		r_p = 5 mils	r_p = 31 mils	r_p = 125 mils
4	0.213	23	146	590
5	0.198	25	157	630
6	0.165	30	190	760
7	0.135	37	230	925

The equilibrium values of electron density and gas temperature behind the incident shock are shown in Figs. 6 and 7 as a function of shock speed. Over the range of shock speeds and pressures that were used, the electron density varied from about 10^{10} to 10^{14} elec/cc, and the gas temperature varied from 2500° to 6000°K.

Due to ablation products from the dielectric liner in the driver section, a sooty deposit was carried down the tube, covering the walls and the probes. It was therefore necessary to clean the probes by lightly rubbing them with fine emory cloth and washing them in alcohol after each shot to ensure reliable measurements.

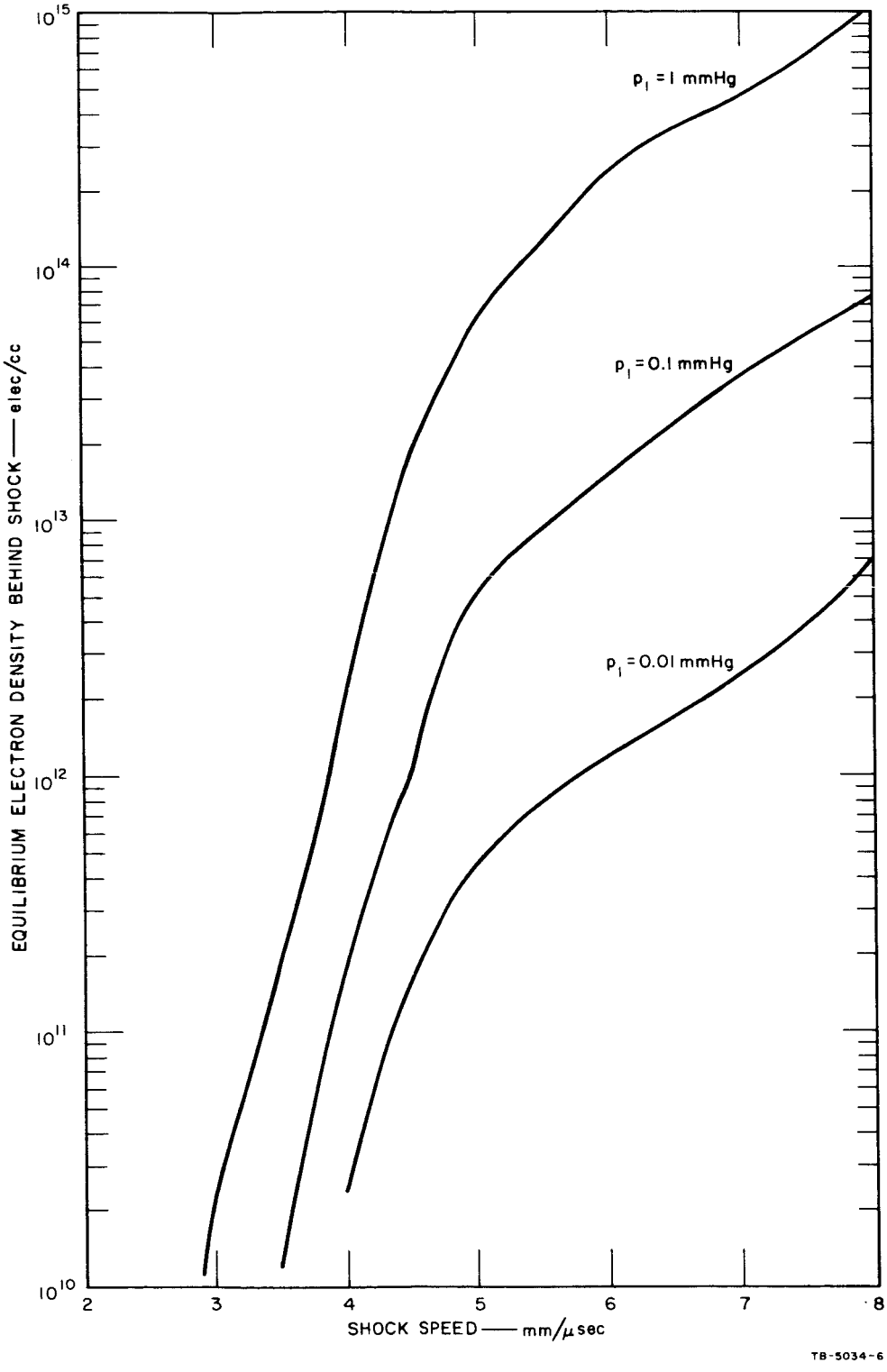

FIG. 6 EQUILIBRIUM VALUE OF ELECTRON DENSITY BEHIND A NORMAL SHOCK AS A FUNCTION OF SHOCK VELOCITY

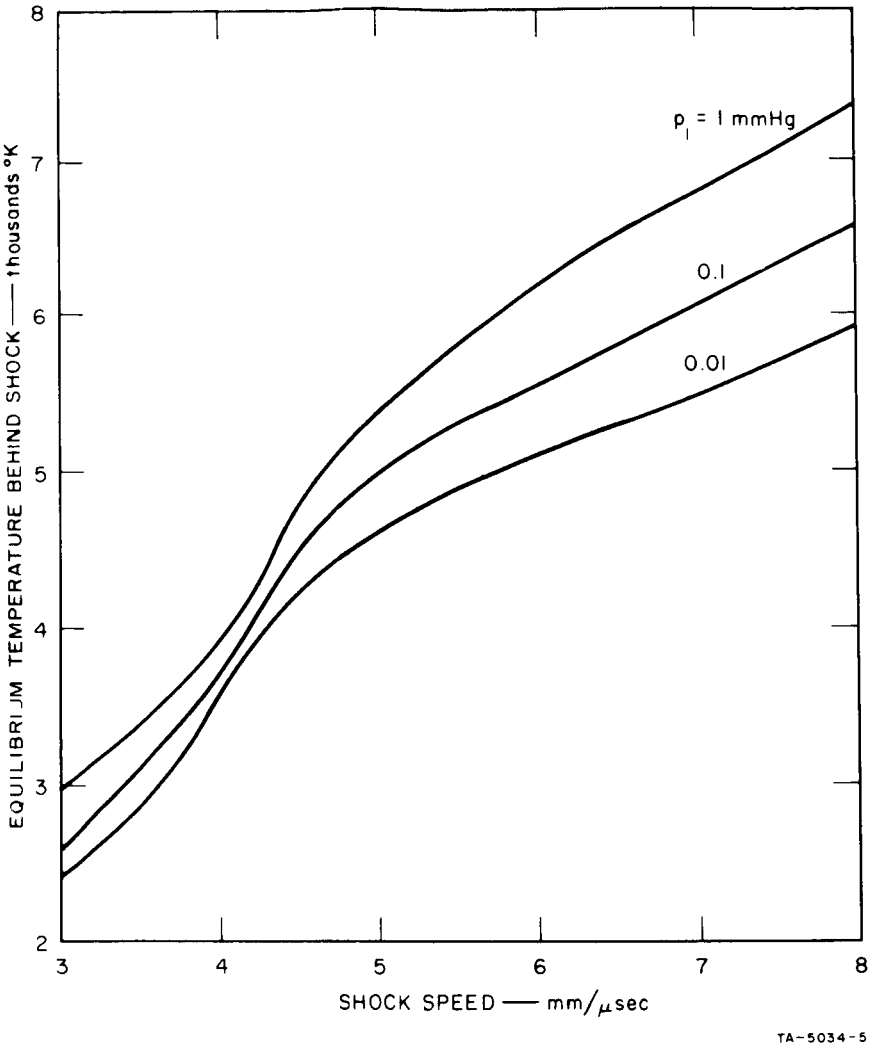

FIG. 7 EQUILIBRIUM VALUE OF GAS TEMPERATURE BEHIND A NORMAL SHOCK AS A FUNCTION OF SHOCK VELOCITY

Tests were made to determine whether the electron density in the slug behind the shock front was the equilibrium value. These tests are described in the appendix. The results showed that equilibrium electron densities were obtained at 1 mmHg even after the tube was fired 40 times without cleaning. Since the electron density is such a sensitive function of gas temperature and impurity level, it was concluded that if the electron density was the equilibrium value, it was likely that the other gas properties were also in equilibrium. At 0.1 mmHg the electron density was below equilibrium by as much as an order of magnitude

if the tube was not properly cleaned. However, it took several shots before the deviation from equilibrium became significant, therefore cleaning after every shot was not required.

Measurements were made with a fixed bias voltage of -15 volts, applied to the cylindrical probe with respect to the shock tube wall. This value was judged sufficiently negative to ensure operation in the ion saturation portion of the current-voltage characteristic. This region of operation has been found to be the most reliable for measurements of electron density in a variety of laboratory plasmas (electromagnetic shock tubes, flames, and dc and RF discharges). The electron saturation current has often been found to give erroneously low readings, depending on the type of plasma. Although it is desirable to have information about the entire current-voltage characteristic for probes in flowing plasmas, it was decided that in the time available more would be learned from fixed-bias, saturated-ion-current measurements.

The circuit diagram for a probe is shown in Fig. 8. The resistor was selected such that the drop across it was small compared to 15 volts.

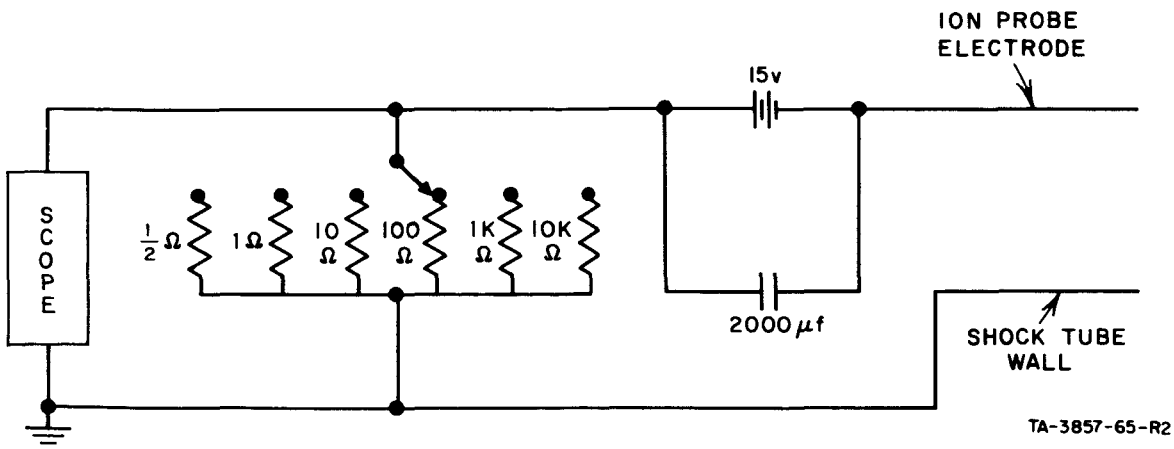

FIG. 8 ION PROBE CIRCUITRY

The probe currents were developed across the resistor and then fed into about 30 feet of RG 58/U cable, which has about 30 μμfd/ft capacitance. The RC time constant resulting from this combination of resistance and capacitance was always less than a microsecond, and most of the time less than 0.1 μsec.

The tests were made with many probes at a single station. In order to be certain that there was no coupling or interference between the probes, all of which had a common ground in the shock-tube wall, tests were run both with a single probe and with many probes at the same station. There was no discernible difference between the two conditions.

B. EXPERIMENTAL RESULTS

1. Cylindrical Probes

A typical probe response is shown in the upper trace of Fig. 9. When the shock arrives there is an abrupt rise in current to a level that

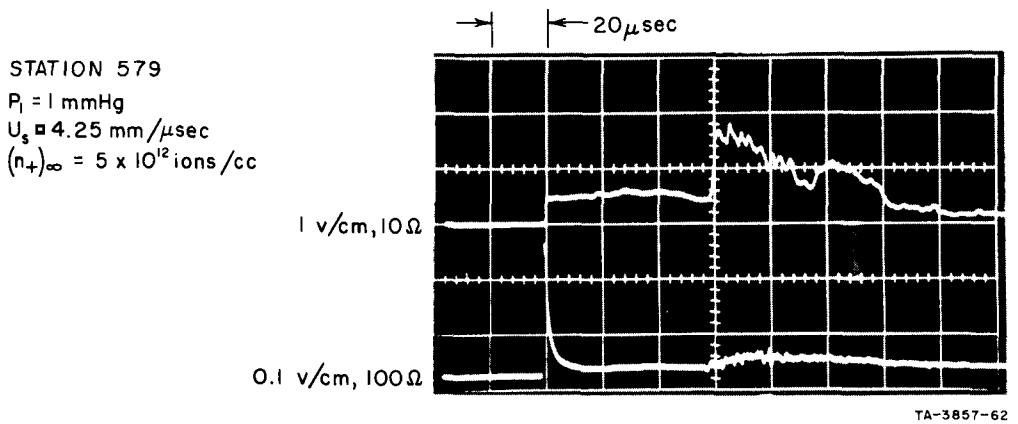

FIG. 9 TYPICAL FREE-STREAM ION PROBE RESPONSE
Upper Trace: Free-Stream Probe
Lower Trace: Flush Probe

stays approximately constant until the contact surface arrives, at which time the current rises sharply and becomes rather erratic. No attempt was made to study the rise in electron density with time across the shock front, although at the lower shock speeds the ionization rise time could be measured. Probes would be an excellent tool for such a study, and would enable information on rate constants to be determined.

The results from the measurements have been reduced to a value of electron density by assuming that the measured current is attributable to collection of the incident flux by the projected area of the probe. This is the case when $a/r_p \approx 1$ and the flow is free-molecular. The

relation between electron density and current that was used is:

$$n_+ = \frac{I_+}{e\, v_f\, d\, L}$$

where I_+ is the measured current and v_f is the shock velocity.

The flow behind the incident shock is less than the shock velocity by a factor of less than 10 percent and varies slowly with shock strength. For ease of data reduction we have used the shock speed rather than the actual flow speed behind the shock.

Over most of the range of electron density the sheath was no larger than the probe radius, but for p_i = 1 mmHg the flow was not free-molecular. We therefore did not expect the current to reach the probe with velocity v_f, but with a somewhat slower velocity, corresponding to the temperature of the electrons behind the shock formed around the probe. However, we have calculated a value of n_+ from the above equation and reduced all of the data in this way simply to have a uniform basis for comparison and some idea of the electron densities measured at the sheath edge. If, in fact, the proper velocity is some fraction of v_f, this should only change the results by a scale factor. If the current is attributable to thermal energy, and so drifts into the probe around the entire circumference rather than only the portion facing the flow, there is a correction of only $\pi/4$.

a. Results at 1 mmHg

The 1-mmHg results are plotted in Fig. 10 in the form of the ratio of the inferred value of n_+ to n_{eq} (the equilibrium value) as a function of n_{eq}. The equilibrium value is determined from the measured value of the shock velocity. Although there is some scatter of points, especially for the 0.01- X 1/4-inch probe at the lower electron densities, a clear pattern is discernible in the data.

None of the probes yield a horizontal line, which would indicate a linear relation between n_+ and n_{eq}. All of them are

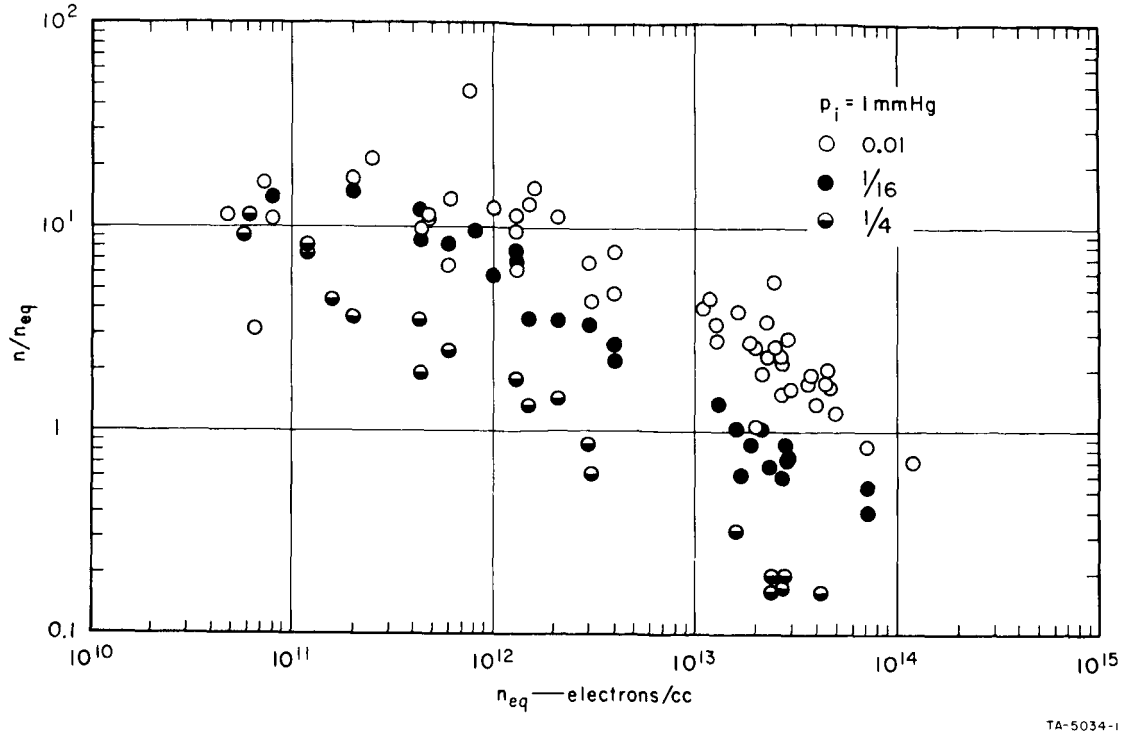

FIG. 10 n_+/n_{eq} AS A FUNCTION OF n_{eq}, p_1 = 1 mmHg

approximately straight lines on log-log paper, with a value which decreases with increasing values of n_{eq}. This relation may be expressed approximately by $n_+/n_{eq} \propto n_{eq}^{-2/3}$, which means that the value of n_+ increases only with $n_{eq}^{1/3}$. In other words, the probe is much less sensitive to the incident electron density than when it is free-molecular.

The value of the ratio is both greater and smaller than unity, although too much significance should not be attached to this fact. If the particles are being collected at a much slower velocity than v_f, then the inferred values of n_+, and hence the ratio n_+/n_{eq}, would be higher.

It is clear from these results that the cylindrical probes for high r_p/λ_2 are disturbing the flow and not simply sampling the incident flow. The error in assuming that the probe operated as if it were free-molecular is as large as plus and minus one order of magnitude over the range of the measurements.

b. Probe Current as a Function of Angle

In order to determine whether the current was indeed being collected only on the side facing the flow, and in proportion to the projected area, when r_p/λ_2 was large, the following experiment was performed.

A 7/16-inch diameter polystyrene rod was made the base of a four-electrode probe, as sketched in Fig. 11. Each electrode was run as a separate probe, with the shock-tube wall as the common electrode for all probes. Currents were measured on each electrode for different rotational settings of the probe with respect to the flow velocity. In this way sufficient data were collected to enable construction of a plot of current as a function of θ, the angle between the flow velocity and the normal to the probe surface. A set of such measurements was made at p_1 = 1 mmHg and a shock velocity of 3.5 mm/μsec; the results are shown in Fig. 12. In this figure the current has been normalized to the current collected when θ = 0 degrees. Most of the current was collected by the portion of the probe facing the flow ($-90^\circ \leq \theta \leq 90^\circ$). The current collected at any angle on the shadow side ($\pm 90^\circ \leq \theta \leq 180^\circ$) was less than 10 percent of the current at θ = 0 degrees.

The current collected on the "illuminated" side varied approximately as the cosine of θ. This is the same sort of variation that one would observe if the probe were free-molecular, although this is certainly not the case. Following Hoegy and Brace[8] we calculated that the value of current at $\theta = \pm 90$ degrees would be about 10 percent of the value at θ = 0 degrees for a value of $v_f/v_+ = 3$. Thus, the form of the current distribution around the probe is similar to that for the free-molecular case, although the level is different. In any case, these measurements demonstrated that the assumption that the current is collected by the projected area of the probe is a good one.

c. Results at 0.1 mmHg

Measurements were made at a pressure of 0.1 mmHg with the same set of cylindrical probes used for the measurements at 1 mmHg.

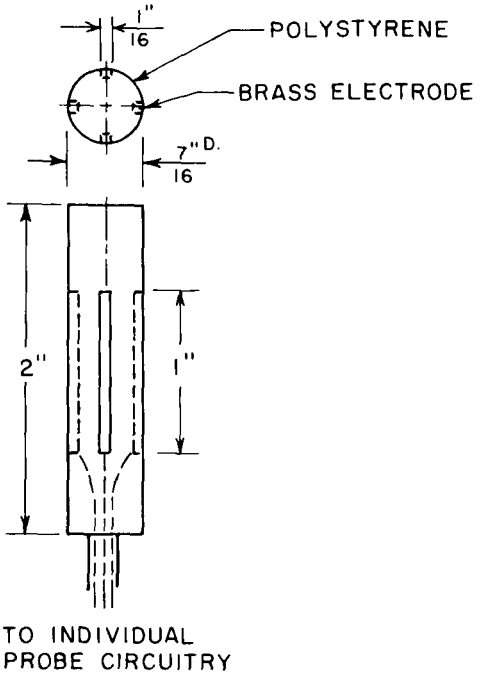

FIG. 11 FOUR-ELECTRODE PROBE CONFIGURATION

As described in the appendix, measurements at 0.1 mmHg pressure with a 0.01- × 1/4-inch probe checked quite well with the results from a 33-Gc microwave interferometer over the electron density range of 4×10^{11} to 4×10^{12} elec/cc, when the probe current was interpreted according to Smetana's formula.[9] This result indicated that the probe was operating under free-molecular conditions, even though it was larger by a factor of three than is allowed for in strictly free-molecular operation. Measurements with a clean shock tube showed that free-molecular operation continued to be true at higher electron densities, with the probe indicating equilibrium electron densities up to almost 10^{14} elec/cc. Since cleaning the tube required so much time, it was decided to use the 0.01- × 1/4-inch probe, which had been checked against microwave measurements, as an indicator of the actual electron density level and as a standard for comparison with the other probes. The tube would then be fired even when it was so dirty that the electron density was other than the equilibrium value. The results of this series of measurements are shown in Fig. 13.

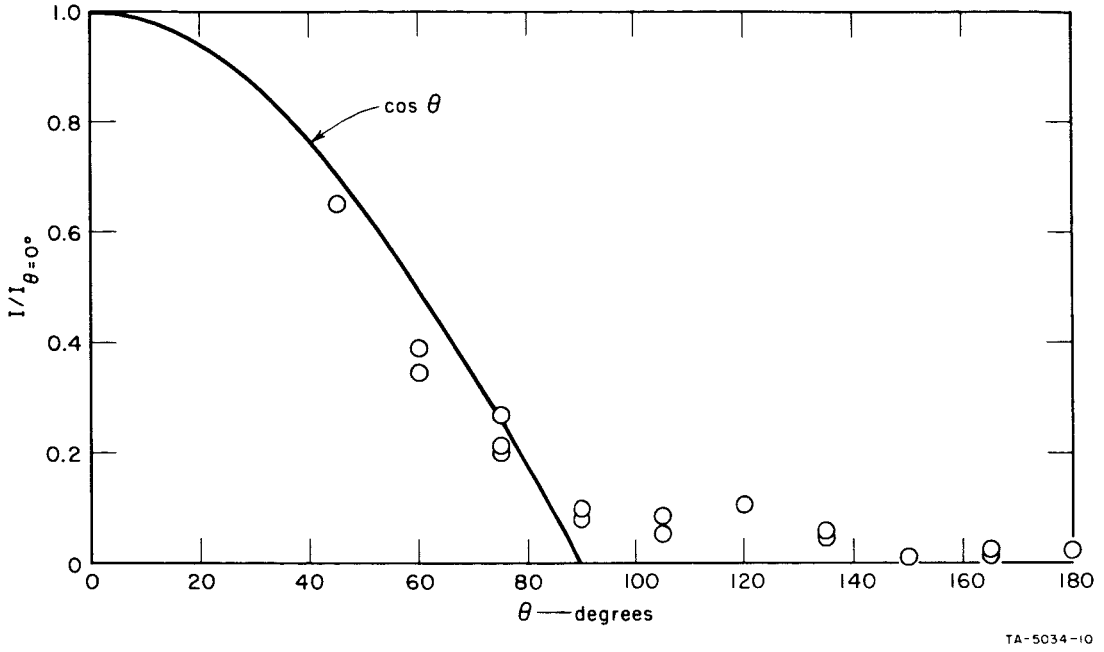

FIG. 12 NORMALIZED CURRENT AS A FUNCTION OF θ

In this figure we have plotted the ratio of n_+, as inferred above, to $n_{0.01}$, the electron density indicated on the 10-mil probe, as a function of the value of $n_{0.01}$. At the lowest value of electron density a sheath correction was necessary for the 0.01 probe, a correction which amounted to a factor of less than three. For the 10-mil probe, which was free-molecular, the curves of Fig. 1 were used with the modifications to account for flow velocity discussed in Sec. II-C.

We may note both similarities and differences between the 1-mmHg and the 0.1-mmHg data. At both pressures, the 1/16- and 1/4-inch diameter probes disturbed the incident plasma, as evidenced by the fact that the ratio of n_+/n_{eq} is not constant with n_{eq}. The ratio at both pressures decreases with increasing values of free-stream electron density, however, at 0.1 mmHg, the 1/16- and 1/4-inch data were not parallel, as was the case at 1 mmHg, and furthermore, the slope for the 1/16-inch probe is less than at 1 mmHg. We shall discuss these similarities and differences more fully in Sec. IV.

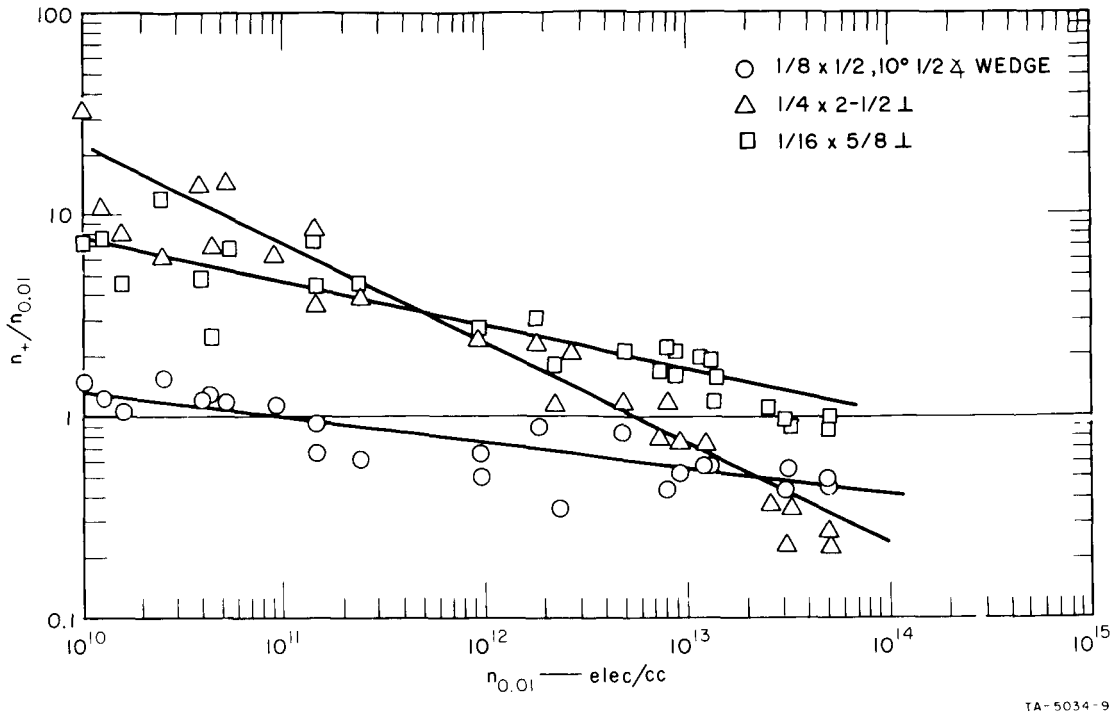

FIG. 13 $n_+/n_{0.01}$ AS A FUNCTION OF $n_{0.01}$, p_1 = 0.1 mmHg

2. Narrow Wedge Probe

Measurements were made at a pressure of 0.1 mmHg with a 10-degree half-angle wedge mounted at zero-degree angle of attack. The wedge dimensions are shown in Fig. 14. The data for the wedge were interpreted using the theory indicated in Sec. II-D. At the lowest electron densities, the sheath was large enough for a modest correction to account for the increased area of current collection.

The data indicate that the plasma flowing over the leading 1/8-inch edge is not significantly different from the incident flow. These data agree with the 0.01-inch probe data within a factor of two over the entire range of electron densities. This indicates that such a probe may be a feasible solution to the problem of constructing a probe that is mechanically strong but that does not disturb the flow. The next logical step is to make measurements with this probe at higher pressures and for other than zero-degree angle of attack.

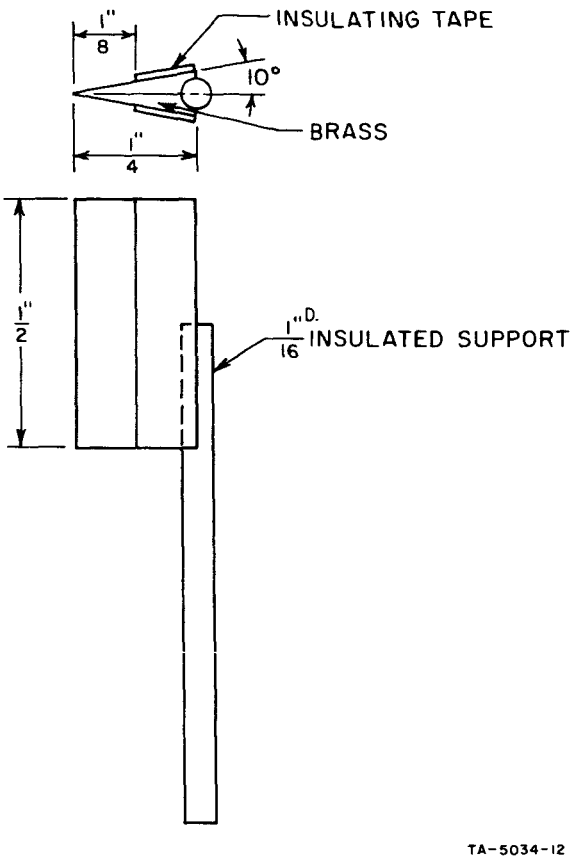

FIG. 14 WEDGE-SHAPED PROBE CONFIGURATION

3. Flush Probes*

The probe geometries tested are shown in Fig. 15. They included a 9.5-mm diameter circular electrode and three strip electrodes of approximate sizes 6.3 × 1.25 mm (HB-1); 7.5 × 1.25 mm (HB-2); and 6.3 × 0.25 mm. Since all probes were connected to a common ground through the oscilloscopes, they were operated as unequal area probes; the shock-tube wall served as the second, circuit-completing electrode.

In Figs. 16 and 17, characteristic flush ion probe responses to widely differing free-stream conditions are shown. Since all the

*Abstracted from SRI Technical Report 26, Project 3857, May 1965.

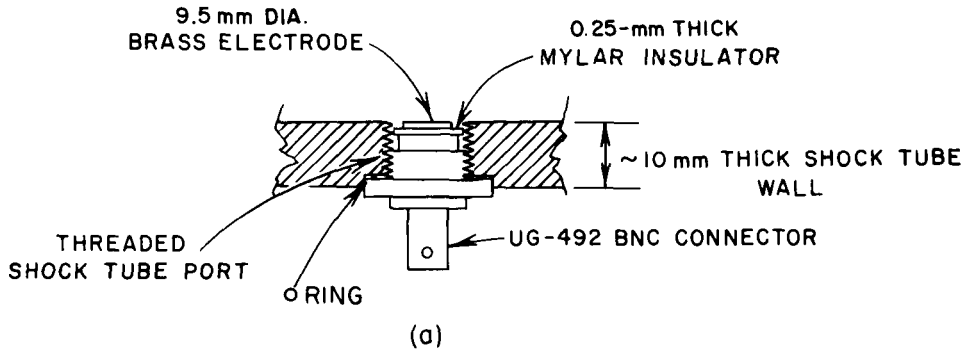

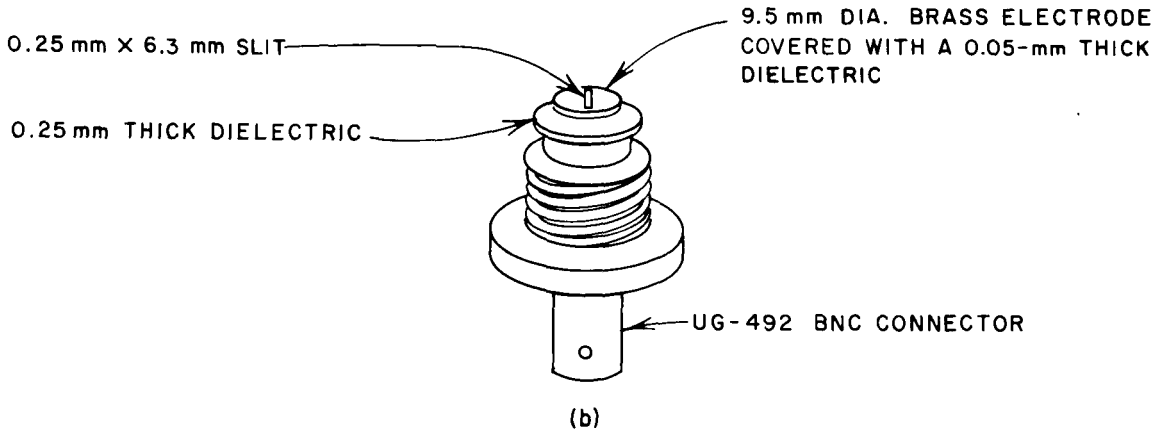

FIG. 15 CONFIGURATIONS OF FLUSH ION PROBES

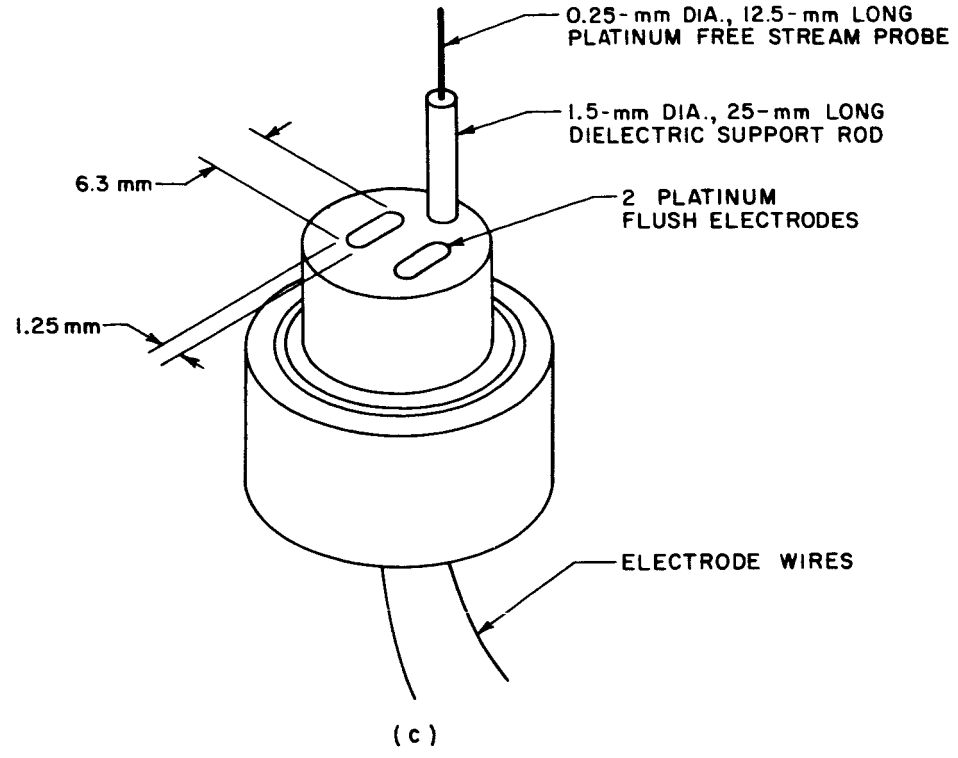

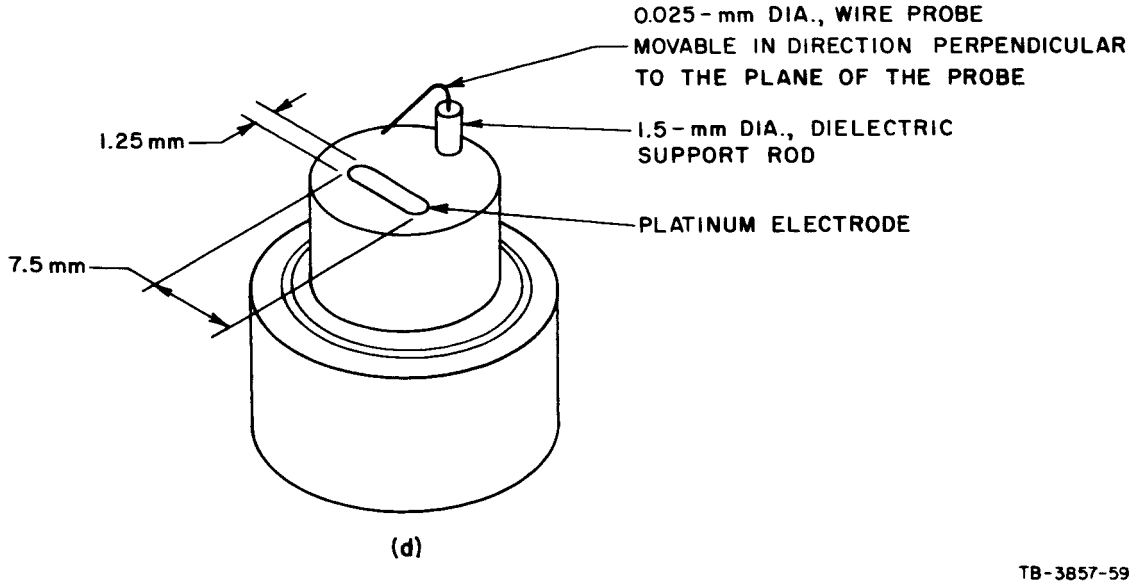

FIG. 15 CONFIGURATIONS OF FLUSH ION PROBES

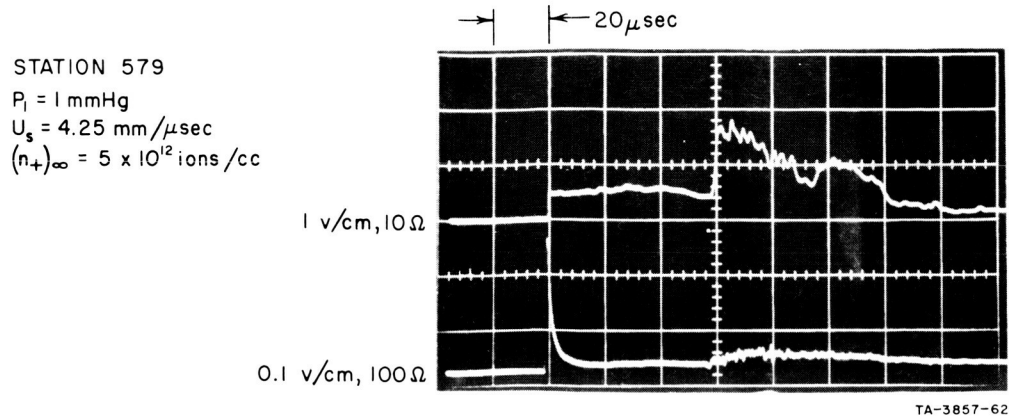

FIG. 16 TYPICAL TIME-RESOLVED RESPONSE OF HB-1 ION PROBE FOR INTERMEDIATE AND HIGH FREE-STREAM DENSITIES
Upper Trace: Free-Stream Probe
Lower Trace: Flush Probe

flush probes indicated similar response characteristics, only the HB-1 probe response is shown. A typical response for intermediate and high free-stream ionization levels is shown in Fig. 16. Note the characteristic current overshoot when the shock arrives. The response of the free-stream ion probe of 0.25-mm diameter and 12.5-mm length is indicated in the same figure. Figure 17 indicates the response of the HB-1 probe to free-stream ion densities about one and one-half orders of magnitude lower (10^{11} ions/cc) than those of Fig. 16. Both the flush probe and the free-stream ion probe show the slow buildup of electron density behind the shock. Note that the overshoot of the flush ion probe is absent in Fig. 17, and that in both figures, corresponding to high and low free-stream electron densities, respectively, the flush-mounted ion probes do not indicate a significant increase in response level upon arrival of the interface, while the free-stream probes always exhibit a substantially increased, fluctuating response. Occasionally, depending on free-stream turbulence, the flush ion probes also show the arrival of the contact surface. In such cases, the flush ion probes follow the free-stream probe response closely.

On Fig. 17 the ionization rise time, which is of the order of 10 μsec, is easily followed by the free-stream probe.

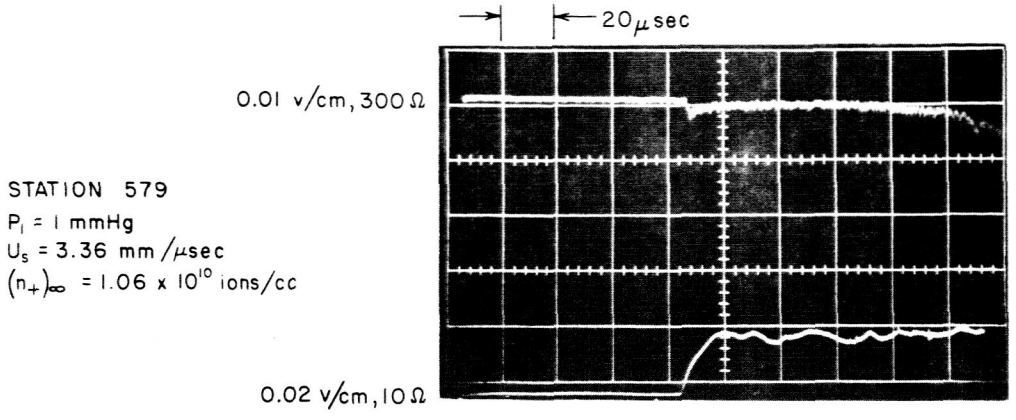

(a) UPPER TRACE: PHOTOMULTIPLIER
LOWER TRACE: FREE-STREAM PROBE

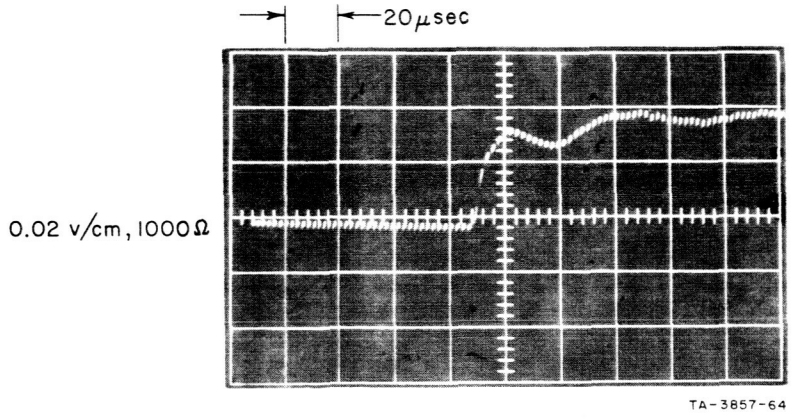

(b) FLUSH PROBE

FIG. 17 TYPICAL TIME-RESOLVED RESPONSE OF HB-1 ION PROBE FOR LOW FREE-STREAM ION DENSITIES

Under turbulent free-stream conditions, as generated by a nonuniform shock wave, the average flush probe response level is substantially increased and exhibits rapid fluctuations (Fig. 18). Compared to a laminar-type probe response for identical theoretical free-stream conditions, the average current level corresponding to turbulent flow is about a factor of two higher.

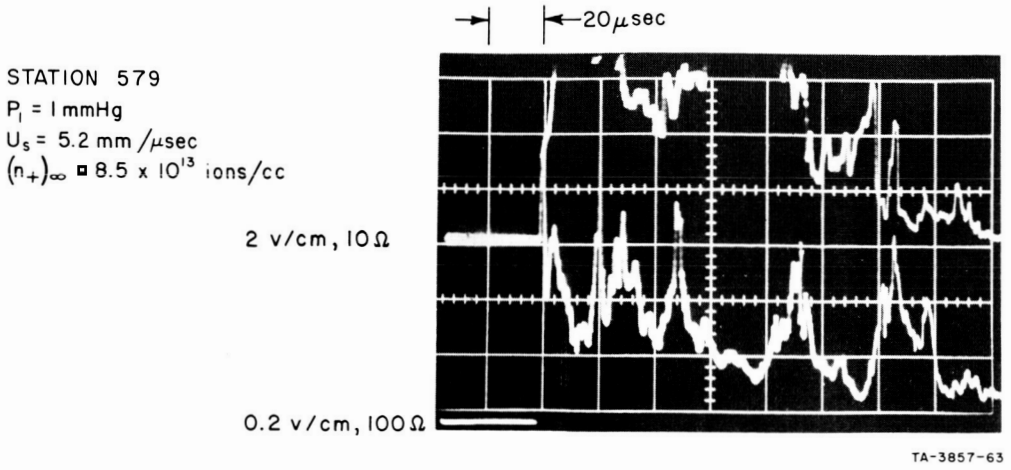

FIG. 18 RESPONSE OF HB-1 ION PROBE TO TURBULENT FREE-STREAM CONDITIONS
Upper Trace: Free-Stream Probe
Lower Trace: Flush Probe

The current overshoot on the flush probes is probably related to the absence of a developed boundary layer immediately behind the shock, the translational temperature overshoot, and the ion density incubation times. The overshoot cannot be attributed to the effects of probe capacity, since no significant correlation between probe area and spike level (or between probe area and probe time response) was found. Also, probes covered with a thin coating of dielectric ($\sim 10\mu$) were more than one order of magnitude reduced in response level, and the transient response was significantly shorter than when observed with the flush ion probes.

The experimental-probe current densities have been plotted against the free-stream ion density (or equivalently, shock velocity) in Fig. 19. Unless the estimated relaxation distances behind the shock front extended further than 10 cm into the test slug,* the data were reduced to the test time corresponding to 10 cm behind the pressure discontinuity.

---

*Here the test slug is defined as the region of shock compressed gas between the shock front and the interface.

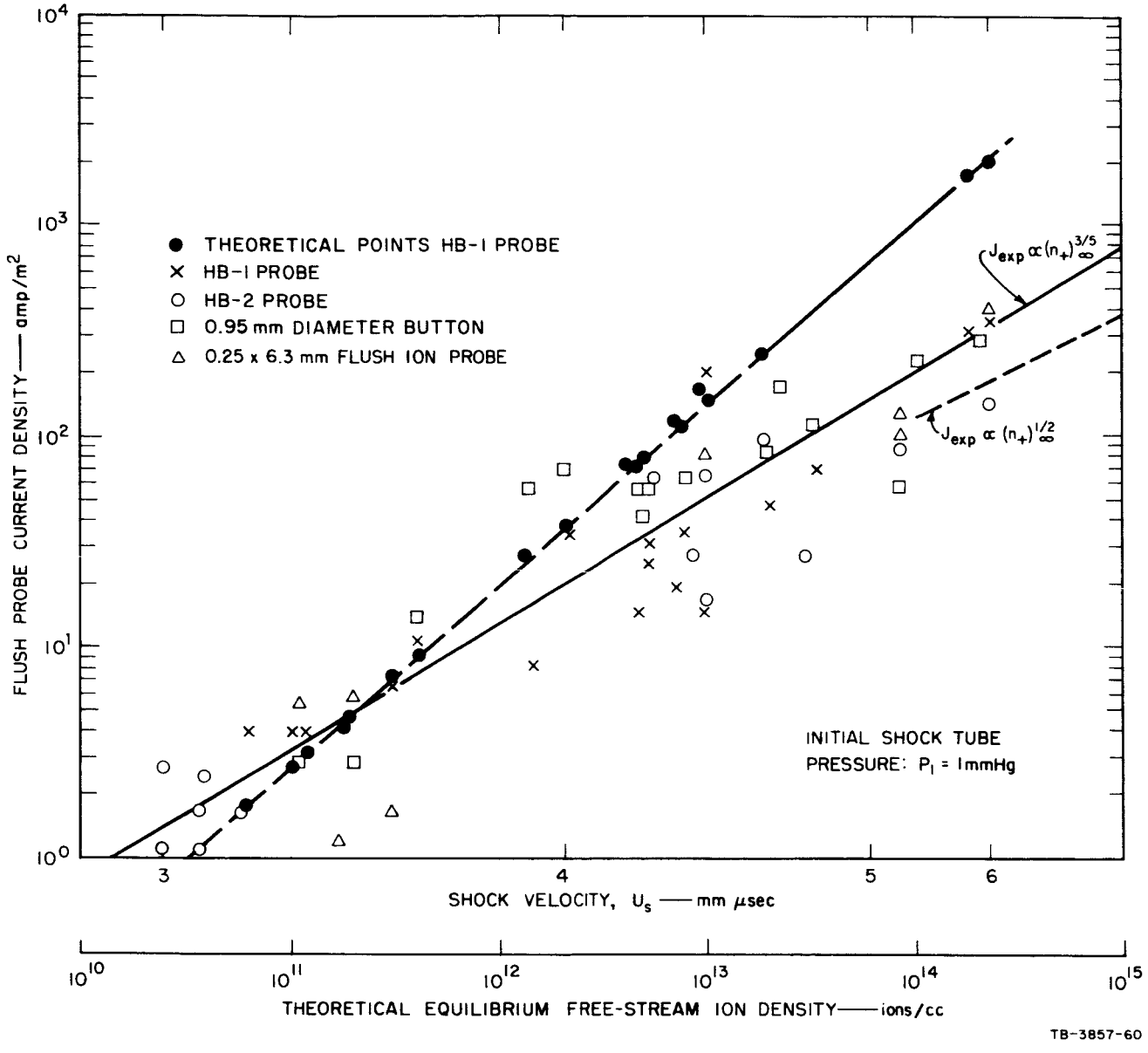

FIG. 19 EXPERIMENTAL AND THEORETICAL FLUSH ION PROBE CURRENT DENSITIES vs. FREE-STREAM EQUILIBRIUM ION DENSITY

When the flush ion probe data were interpreted on the basis of a zero-order probe theory, described in Sec. I-F, it was found that the flush probes indicated ion density levels much closer to free-stream values than had initially been expected. The initial estimates were based on the assumption that the cold gas near the wall was in ionization equilibrium. At the low free-stream ion densities (10^{10} ions/cc),

the ion density inferred from flush probe data was a factor of three lower than the corresponding free-stream value. At the higher free-stream ion densities (10^{14} ions/cc), the flush probe data indicated values about an order of magnitude low.

Presumably because of poor experimental conditions in the unsteady boundary layer, i.e., driver impurities deposited on the shock-tube wall and turbulent free-stream conditions, the spread in experimental data is about one order of magnitude. However, when observing the variation of test data over four orders of magnitude of free-stream ion density, from 10^{10} ions/cc to 10^{14} ions/cc, it becomes evident that for the present experimental conditions, the flush ion probe current level increases with increasing free-stream ion density and is much closer to free-stream values than considerations of ionization equilibrium at the wall would indicate.

If the accumulated data from all probes are considered, the flush probe current varies approximately as

$$J_+ \propto n_+^{3/5} \quad .$$

However, a better fit through the HB-1 and HB-2 probe data, which covered the widest range of free-stream conditions, would yield

$$J_+ \propto n_+^{\frac{1}{2}} \quad .$$

The difference in the power dependence is caused by the fact that the larger (9.5-mm diameter) buttons (used principally at the intermediate free-stream ion densities) seemed to yield higher current densities than probes HB-1 and HB-2 by about a factor of two. However, no definite conclusion can be made at this time, since this difference in current level is well within the experimental data scatter.

Over the range of free-stream conditions covered, from 10^{10} to about 10^{14} ions/cc, it was found that the flush-mounted ion probes sampled the ion density existing at the probe sheath edge. Interpreting

the probe current as $J_+ = n_+ e v_+ / 4$, at the low free-stream ion density levels, the flush-mounted ion probes measured ion density about a factor of three lower than free-stream values. For high free-stream ion densities, the probes indicated ion densities about one order of magnitude reduced from free-stream levels. These results agree well with theoretical expectations based on boundary-layer ion density profiles and sheath dimensions computed by means of the collision-dominated, space-charge-limited diode equation. In addition, considerations of probe theory indicate another means of obtaining boundary-layer ion density profiles from flush probe data. Equation (9) shows that d_s has a strong dependence on the probe potential. Thus, if the probe sheath can be varied by modulating the probe potential, it may be possible to obtain the ion density profile in the boundary layer.

IV SCALING RELATIONS

The measured data presented in the previous section display some striking characteristics. The data at 1 mmHg show that each probe collected current at a rate proportional to $n_{eq}^{\frac{1}{3}}$. Furthermore, the ratio of the proportionality constants for the 1/16- and 1/4-inch probes (the two probes that are clearly in continuum flow at this pressure) is in inverse proportion to the probe radii. That is, at a given shock velocity and initial pressure, the 1/16-inch probe collected four times more current than the 1/4-inch probe. This suggests some sort of scaling that depends upon the product $n_+ r_p$, since this product is constant for the probes considered so far.

In order to investigate the effect of pressure on this scaling relation, we calculated the product $n_+ r_p$ obtained from the measured data at 0.1 mmHg for the 1/4-inch probe (the only probe clearly in the continuum flow regime). In Fig. 20 the results for the data at the two pressures are plotted. In order to get sufficient overlap in the curves we have straight-line extrapolated the 1-mmHg data of Fig. 10 to higher shock velocities. This is a reasonable assumption, since the data exhibited straight-line characteristics over three orders of magnitude in electron density.

From the available data it appears that $n_+ r_p$ is approximately constant, not only with probe radius but also with pressure. If this assumption proved to be true over the whole continuum flow regime, it would be a valuable aid in interpreting probe data obtained under this flow condition. The data at present are suggestive, but they are too scanty to permit a high degree of confidence in predictions at other pressures and probe radii. It is therefore very desirable to study continuum probe operation to clarify the scaling relations.

We have constructed a model which accounts for the measured results; however, it must be realized that the model is somewhat speculative, and further investigation is required to determine its validity. A binary

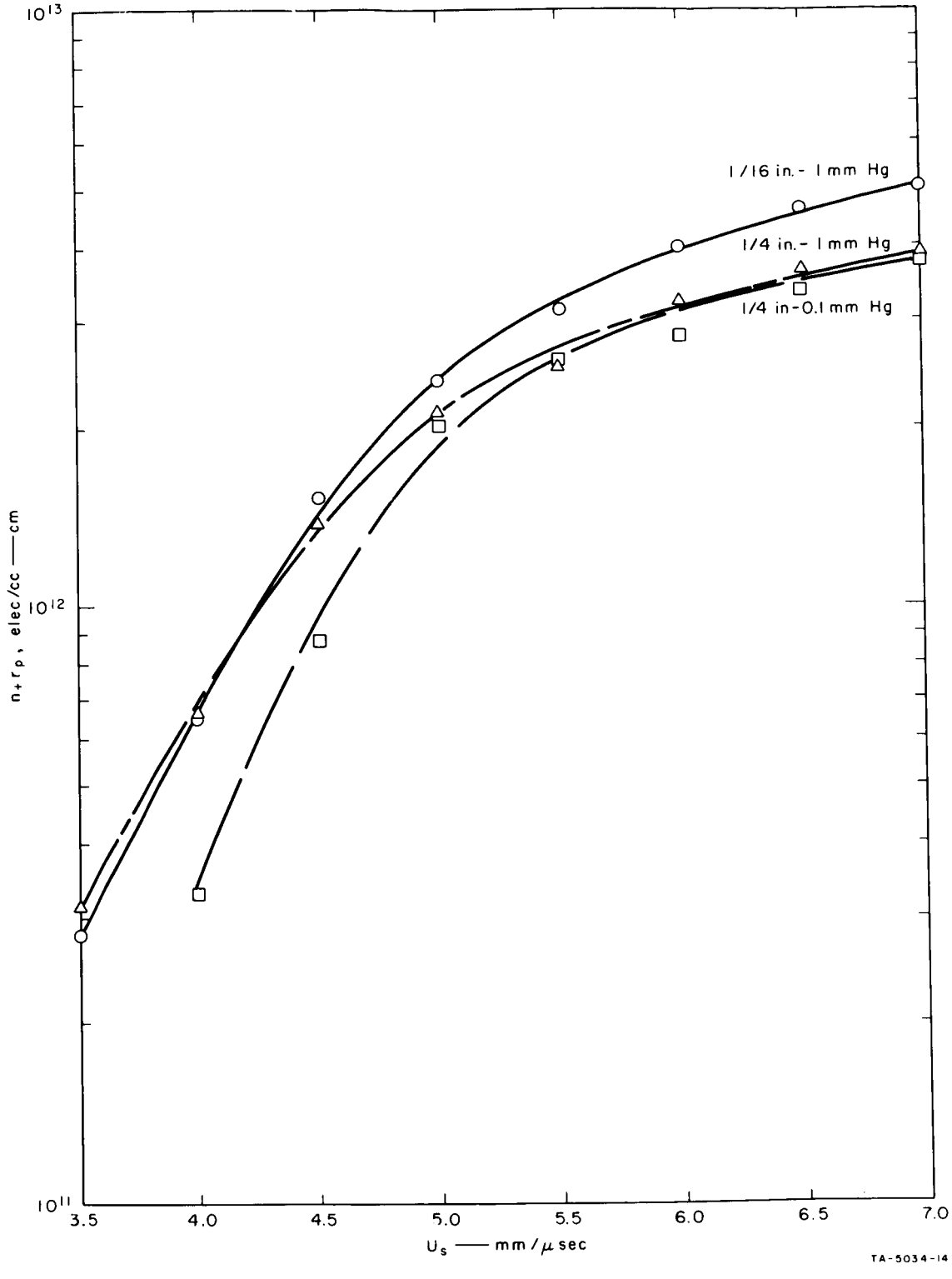

FIG. 20 $n_+ r_p$ AS A FUNCTION OF SHOCK VELOCITY FOR CONTINUUM FLOW

scaling model, for which the ionization flow field would scale if $\rho_2 r_p$ = constant (where ρ_2 is the gas density behind the incident shock), could account for the results obtained with the 1/4-inch probe at 0.1 mmHg and for an extrapolated value (between the 0.01- and the 1/16-inch probe data) for a 0.025-inch probe at 1 mmHg, but it would not shed any light on the relation between data for different sized probes at the same initial gas density. The following model accounts for both probe size and pressure variations.

The flow field is divided into four regions as shown in Fig. 21. Region 1 is the incident flow and has the properties associated with an equilibrium slug of gas behind a normal shock. Region 2 is the shocked region around the probe and extends from the detached shock front to the boundary layer surrounding the probe. Region 3 is the viscous boundary layer, which we shall assume is not in ionization equilibrium. Region 4 is the sheath-edge-to-probe-surface region and is embedded within the boundary layer for the ionization levels under consideration.

When recombination of electrons and ions is important in the boundary layer, the decrease in electron density across the boundary layer to the sheath edge is related to the time required to cross the boundary layer. Adamson points out that to a good approximation the velocity along the stagnation streamline decreases linearly from the shock front to the wall.[14] Using this approximation, calculation of the time for ions to cross the boundary layer has been made.

The velocity at the shock front in region 2 is related to the incident velocity, approximately, by the density jump, so that

$$v_{2s} = (\rho_1/\rho_2)v_1 \quad .$$

For a linear velocity decrease, the velocity at the boundary layer edge is

$$v_{b1} = \frac{d_{b1}}{d_s} v_2$$

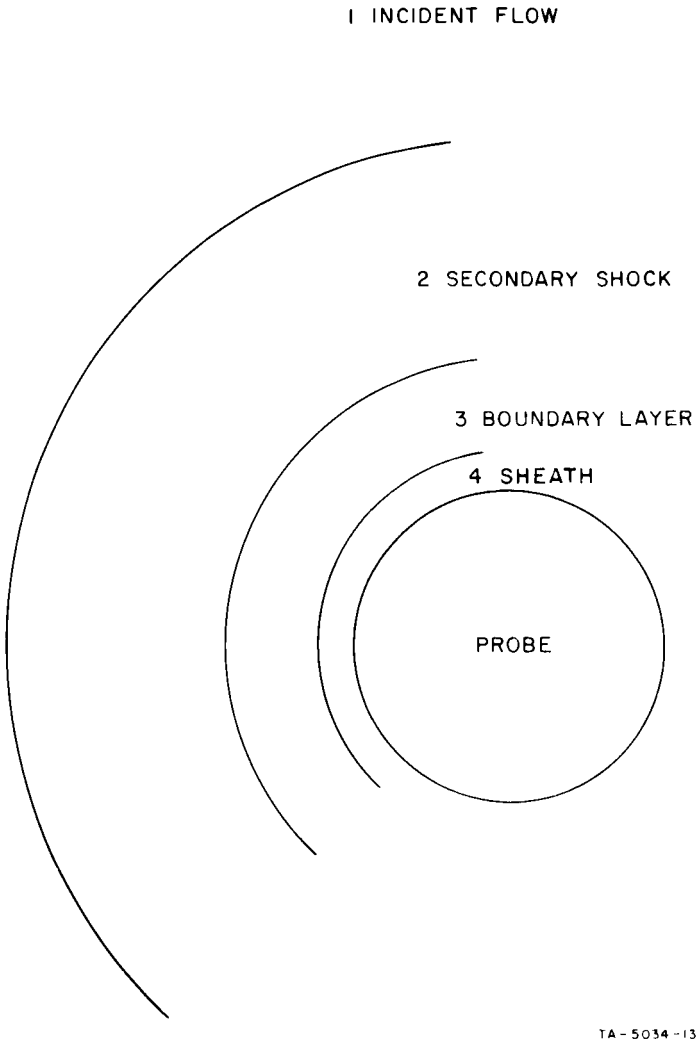

FIG. 21 FLOW FIELD ABOUT A CYLINDRICAL PROBE IN SUPERSONIC CONTINUUM FLOW

where

d_{bl} = boundary layer thickness

d_s = shock detachment distance

v_{bl} = velocity at the boundary layer edge.

The time to cross the boundary layer edge, t_3, is

$$t_3 = 2\, d_{bl}/v_{bl} \quad .$$

This may be related to the incident velocity to give

$$t_3 = \frac{2\, d_s}{(\rho_1/\rho_2)v_1} \quad .$$

Hartsel shows that for the Mach number range with which we are concerned, $d_s \approx 0.4\, r_p$.[15] Substituting this value for d_s in the equation for the transit time, we obtain

$$t_3 = \frac{0.8\, r_p}{(\rho_1/\rho_2)v_1} \quad .$$

For a recombination process, the electron density as a function of time is

$$1/n = 1/n_0 + \alpha t$$

where

n_0 is the electron density at $t = 0$

α is the recombination coefficient.

If recombination is significant, the initial electron density term is negligible and the electron density is

$$n = \frac{1}{\alpha t} \quad .$$

The value of the ion density at the sheath edge may be found by inserting the ion transit time into the recombination equation. Thus,

$$n_{+s} = \frac{(\rho_1/\rho_2)v_1}{0.8\alpha r_p} \quad .$$

Multiplying through by r_p we obtain an expression for $n_{+s}r_p$

$$n_{+s}r_p = \frac{(\rho_1/\rho_2)v_1}{0.8\alpha} \quad .$$

For dissociative recombination, α is dependent only upon temperature. Thus, $n_{+s}r_p$ is independent of r_p, and since ρ_1/ρ_2 is only weakly dependent upon ρ_1, $n_{+s}r_p$ is also independent of ρ_1. This checks with the experimental results.

To check whether recombination is significant, we shall compute n_{+s} at the lowest electron density for which scaling was observed. This will be the most severe test of the importance of recombination.

From Lin and Teare we find that the value of α for recombination of NO^+ and electrons is[16]

$$\alpha = 3\ (10^{-3})\ T^{-3/2} \quad .$$

The uncertainty in α is about three, with experimental results giving higher values. Therefore, for an average temperature of about 5000°K through most of the boundary layer, α is between 1 and 3 (10^{-8}).

For the 1/4-inch probe, at a velocity of 4 mm/μsec, the value of t_3 is 3.75 μsec. Therefore, the calculated value of n_{+s} is between 9 (10^{12}) and 2.7 (10^{13}) elec/cc.

The experimental results under these conditions showed that the probe indicated an ion density 1.5 times the equilibrium value when the probe current was considered attributable to flow velocity. This gives an ion density of 3 (10^{12}) elec/cc. However, the ions do not enter the sheath with the incident flow velocity, but with the much slower thermal velocity. Because of cooling in the boundary layer, the temperature at

the sheath edge is about 2000°K, therefore, the inferred ion density is about four times higher than indicated above. This gives a value of $n_{+s} \approx 1.2\ (10^{13})$ elec/cc, which checks fairly well with the recombination hypothesis.

V CONCLUSIONS AND FUTURE WORK

Some conclusions which can be drawn from the work presented in the previous sections of this report are given below. Extensions of the work along several lines are also indicated.

1. The theory of cylindrical electrostatic probes in flowing plasmas outlined in Sec. II-C has been verified for the case in which the sheath thickness is small compared to the probe radius ($a/r_p \approx 1$). Extension of this work to the case in which $a/r_p \gg 1$, which would correspond to lower electron densities, would be a valuable addition to our understanding of this type of probe operation. The assumption that the sheath shape is not changed by flow will be more critical for $a/r_p \gg 1$. Also, the effect of collisions in the sheath will be more dominant.

2. The experimental results show that the free-molecular theory for flowing plasmas gives accurate results for probe radii as large as three times the neutral-neutral mean free path of the flowing gas. Significant deviations from free-molecular operation were noted when the ratio of probe radius to mean free path was greater than 20. The transition between $r_p/\lambda_2 = 3$ and $r_p/\lambda_2 = 20$ was not measured. It would be desirable to make measurements which would cover the transition from free-molecular to continuum flow. It is also of interest to know the maximum value of r_p/λ_2 for which free-molecular theory will give results accurate to a specified level. Such information could be obtained from measurements in the transition region.

3. Cylindrical probes operating in the continuum region (say, $r_p/\lambda_2 > 30$) do not collect current at a rate proportional to the electron density of the incident plasma. The electron density indicated by such probes varied as only the 1/3 power of the incident electron density; that is, $n_{+\ probe} \propto (n_{incident})^{\frac{1}{3}}$. Cylindrical probes are thus much less sensitive instruments for measuring electron densities in a flowing plasma than free-molecular probes.

4. For probes operating in continuum flow over the range of pressures and shock velocities that were measured, it appears that the product $n_{+s} r_p$ is a constant with respect to initial pressure and probe radius and is only a function of shock velocity. The value of n_{+s} is that inferred from the relation $I_+ = n_{+s}\ e\ v_f\ 2r_p\ L$. Measurements should be made over a wider range of probe sizes and initial pressures to investigate the apparent constancy of $n_{+s} r_p$ with these parameters. It appears that the constancy of $n_{+s} r_p$ can be accounted for by recombination in the boundary layer.

5. A narrow wedge-shaped structure at zero-degree angle of attack, with base dimensions of 30 mean free paths, collected current as a free-molecular probe. It thus appears that such probes will be useful for measurements on re-entry vehicles, since they incorporate mechanical strength with good probe performance. The angle of attack will not, in general, be zero degrees, so that it is necessary that these structures be tested at other angles of attack. It is to be expected that their performance as probes will deteriorate at large angles of attack, but it is desirable to have a measure of the range of angles of attack over which

such probes can work with a specified degree of accuracy. The present measurements were limited to an initial pressure of 0.1 mmHg. Measurements should be performed at higher pressures to verify the capability of such probes to sample the incident plasma accurately.

6. Flush probe measurements indicated that these probes sample the electron density at the sheath edge. Due to nonequilibrium effects in the boundary layer, the electron density at the sheath edge may be much closer to the free-stream values than an equilibrium theory would predict. There is a possibility that the electron density profile near the probe may be measured by varying the probe potential. The distance out from the surface to which this can be effectively done is a function of the free-stream electron density, the distance decreasing as the electron density increases.

7. All the measurements presented in this report were made at a fixed bias of -15 volts. Measurements should be made of the entire current-voltage characteristic to determine the ability of such probes to yield measurements of temperature, as well as to see if the ion current characteristic is behaving as predicted by theory.

8. It has been noted that under certain conditions probe surfaces may become contaminated and give erroneous measurements unless properly cleaned. It is not clear whether the effect is due to oxidation on the surface or the deposit of some material that was in the plasma. Since probes may be used on re-entry vehicles which ablate material into the flow field, it is important to know how such materials would affect probe operation. This area requires a systematic investigation.

APPENDIX

PRESSURE-DRIVEN SHOCK TUBE

The laboratory simulation of probe operation associated with planetary re-entry conditions necessitates the existence of a high-velocity plasma. For short test times, the arc-driven shock tube can provide strong shocks and equilibrium plasmas moving with velocities up to about 40,000 ft/sec. One general advantage of shock-tube testing is that, if equilibrium test conditions exist in the test slug, the gas properties are a function only of shock velocity. Thus, an accurate measurement of shock velocity yields all equilibrium gas properties.

1. Description of the Equipment

The shock tube used in these studies is of the arc-driven type and is modeled after the design of Camm and Rose.[17] A schematic of the shock tube is presented in Fig. A-1. Figure A-2 shows a cross section through the shock-tube driver. The driver is 1-1/2-inches in diameter and 12 inches long. The driver is connected to the 12-inch diameter driven tube by means of a 54-inch long circular transition section. The length of the driven tube has recently been increased from 25 to 36 feet.

The energy source is a 100-kilojoule capacitor bank, which is triggered by an exploding wire technique.

Shock velocity is measured by a series of flush probes mounted in the tube walls. The probe current develops a voltage across a resistor. This voltage is then differentiated to give a spike in voltage when the ionization front passes the probe. The voltage spike is applied to the vertical plates of a raster oscilloscope (see Fig. A-3), and the time for the shock to travel a known distance is measured from the oscilloscope in terms of the time between spikes. The accuracy with which velocity is measured is estimated to be about 2 percent.

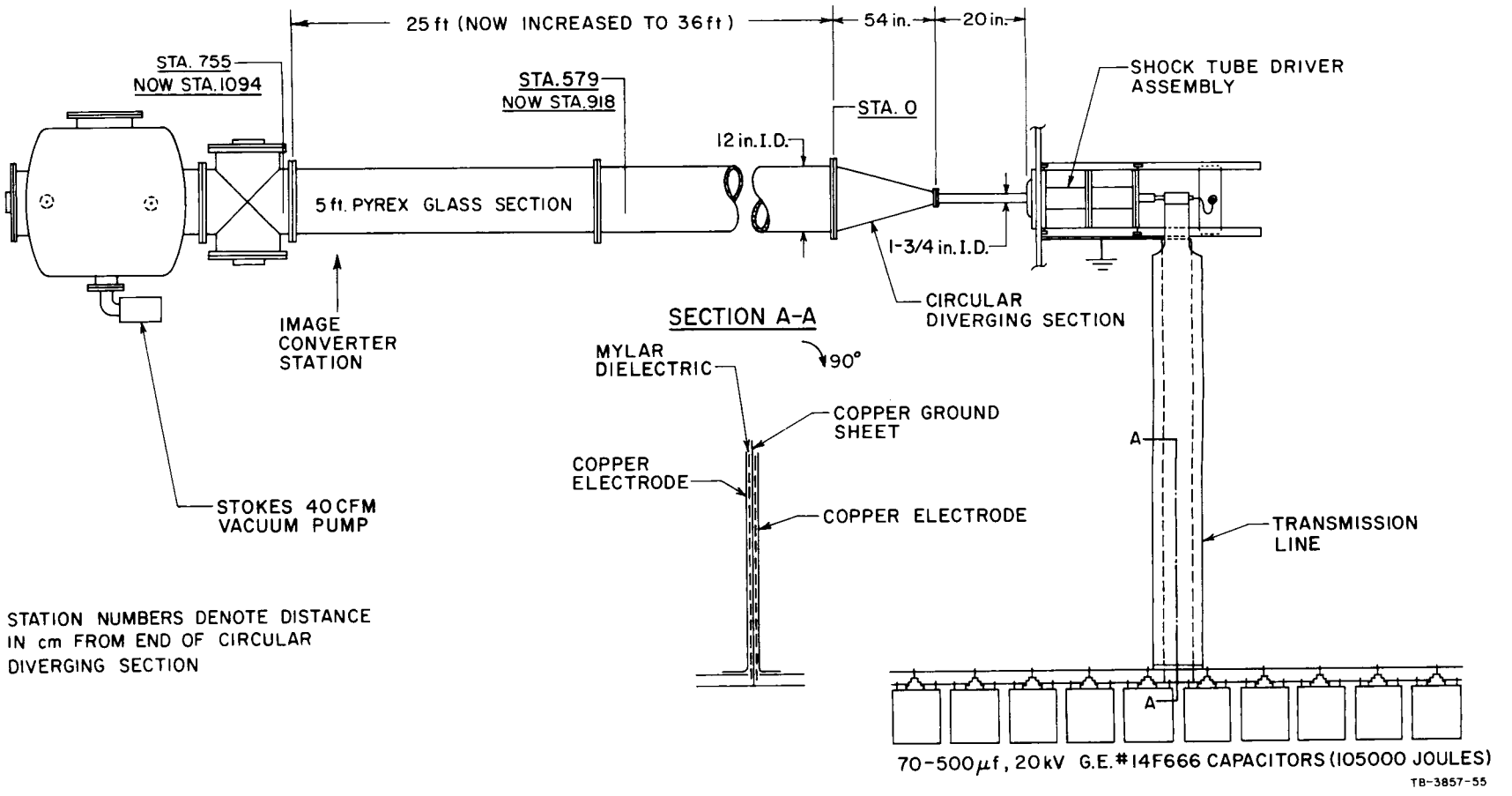

FIG. A-1 SCHEMATIC LAYOUT OF PRESSURE-DRIVEN, ARC-HEATED SHOCK TUBE

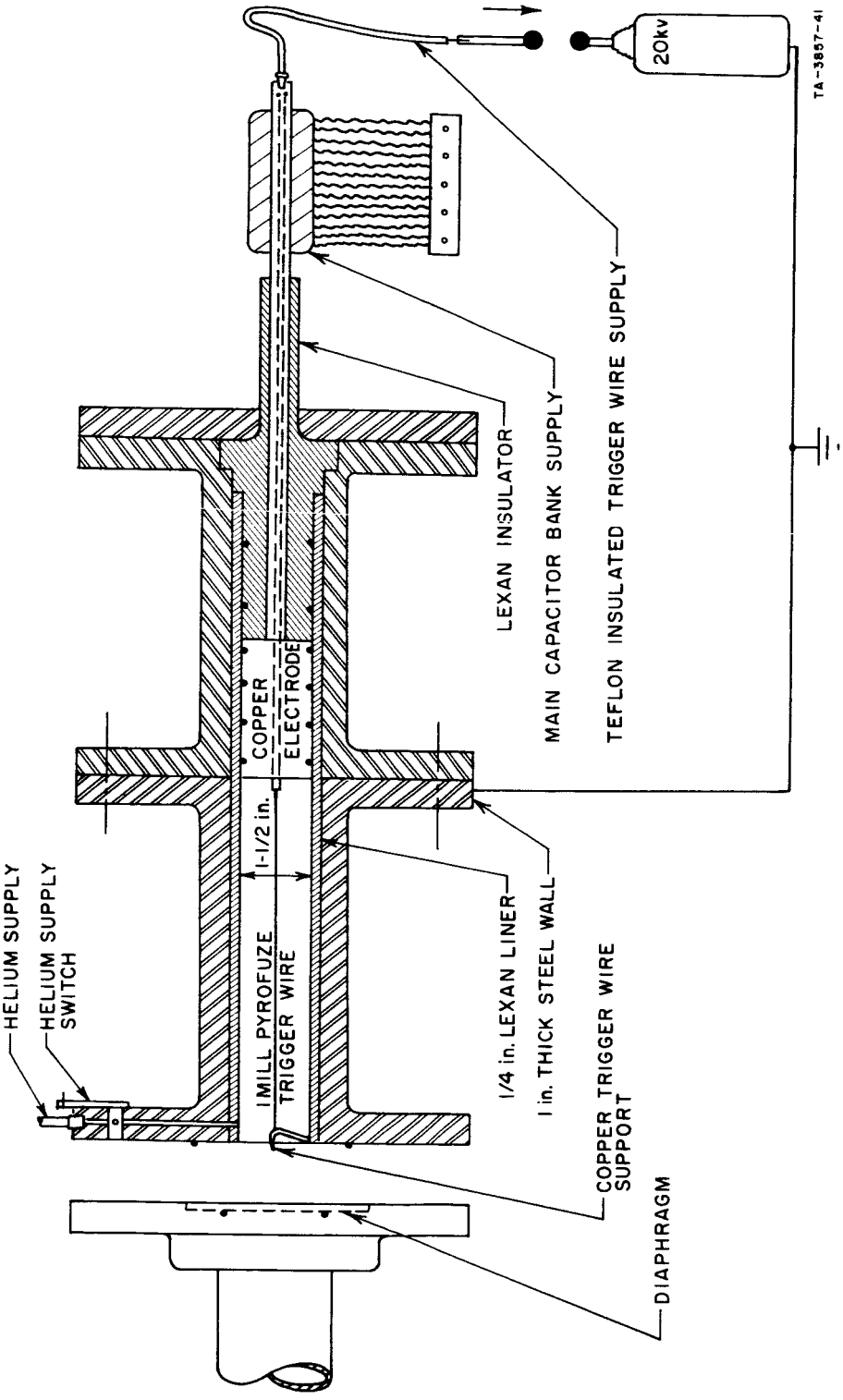

FIG. A-2 CROSS SECTION OF SHOCK-TUBE DRIVER

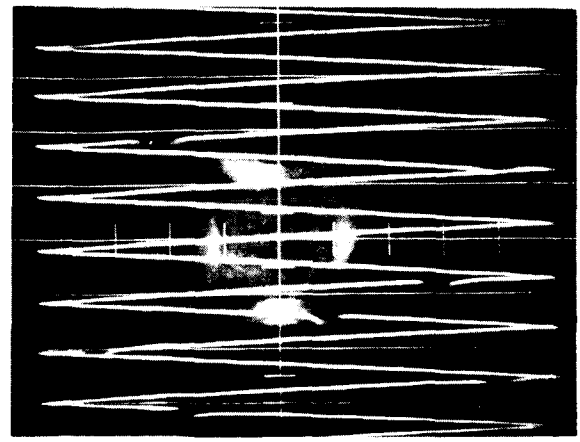

FIG. A-3 SHOCK VELOCITY MEASUREMENT ON RASTER SCOPE

Shock velocity versus capacitor-energy input into the driver is shown in Fig. A-4. To date the shock tube has been tested at 1 mmHg and 0.1 mmHg initial pressures. The capacitor bank voltage variations ranged from 7 kv to 15 kv. It is perhaps worth mentioning that our particular driver triggering system has permitted us to break down the driver gas at very low voltages, say 6.5 kv, and 200-psi driver pressures without difficulties.

2. Test for Equilibrium

Measurements were made at 0.1 and 1.0 mmHg to check that the slug of ionized gas was indeed in ionization equilibrium. This was done by phase measurements made at 33 Gc with a microwave interferometer. The transmission path was between a pair of horns spaced 2 inches apart and located symmetrically about the tube axis (see Fig. A-5). The horns were mounted so that their apertures were flush with the surface of the plates, 2 inches from the plate leading edge. The plates were 2 inches wide and 3 inches long, with sharp tapers at their leading edges to minimize flow disturbances. The horn apertures were covered with Mylar tape.

Using this system, electron densities were checked over the range of 10^{10} to 3×10^{12} elec/cc at 1 mmHg with the results shown in Fig. A-6.

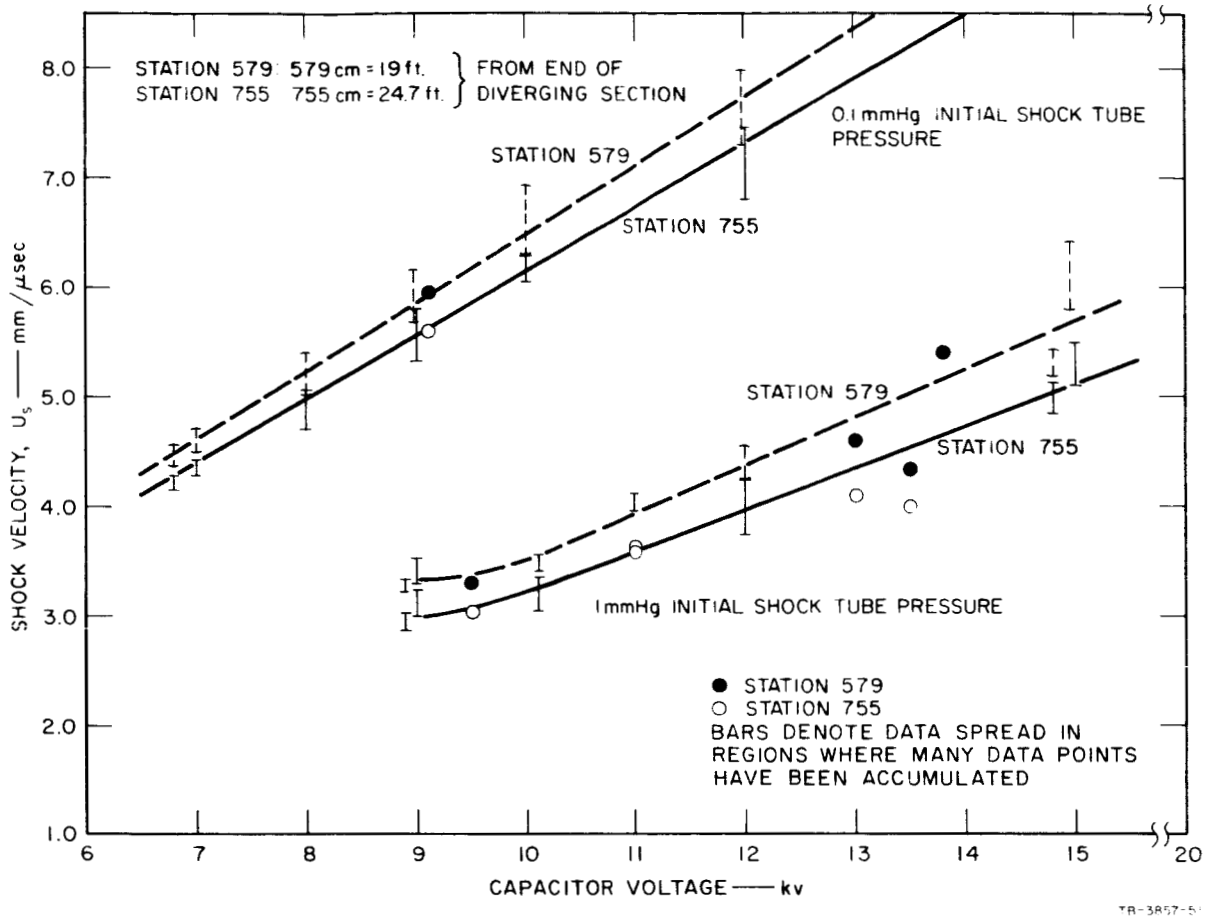

FIG. A-4 SHOCK VELOCITY vs. CAPACITOR VOLTAGE FOR PRESSURE-DRIVEN, ARC-HEATED SHOCK TUBE

The rms difference between the electron densities inferred from the interferometer measurements and the values of the equilibrium electron densities calculated from the measured data on shock velocity was less than 30 percent. These results were obtained with the tube fired over thirty times without cleaning.

The tube was operated with dry air as well as with ordinary room air. No significant difference was detectable, either with probes or with the interferometer; neither was a change in agreement with equilibrium calculations detected.

Measurements made at 0.1 mmHg showed more sensitivity to tube cleanliness when fired at slower velocities. Measurements made with

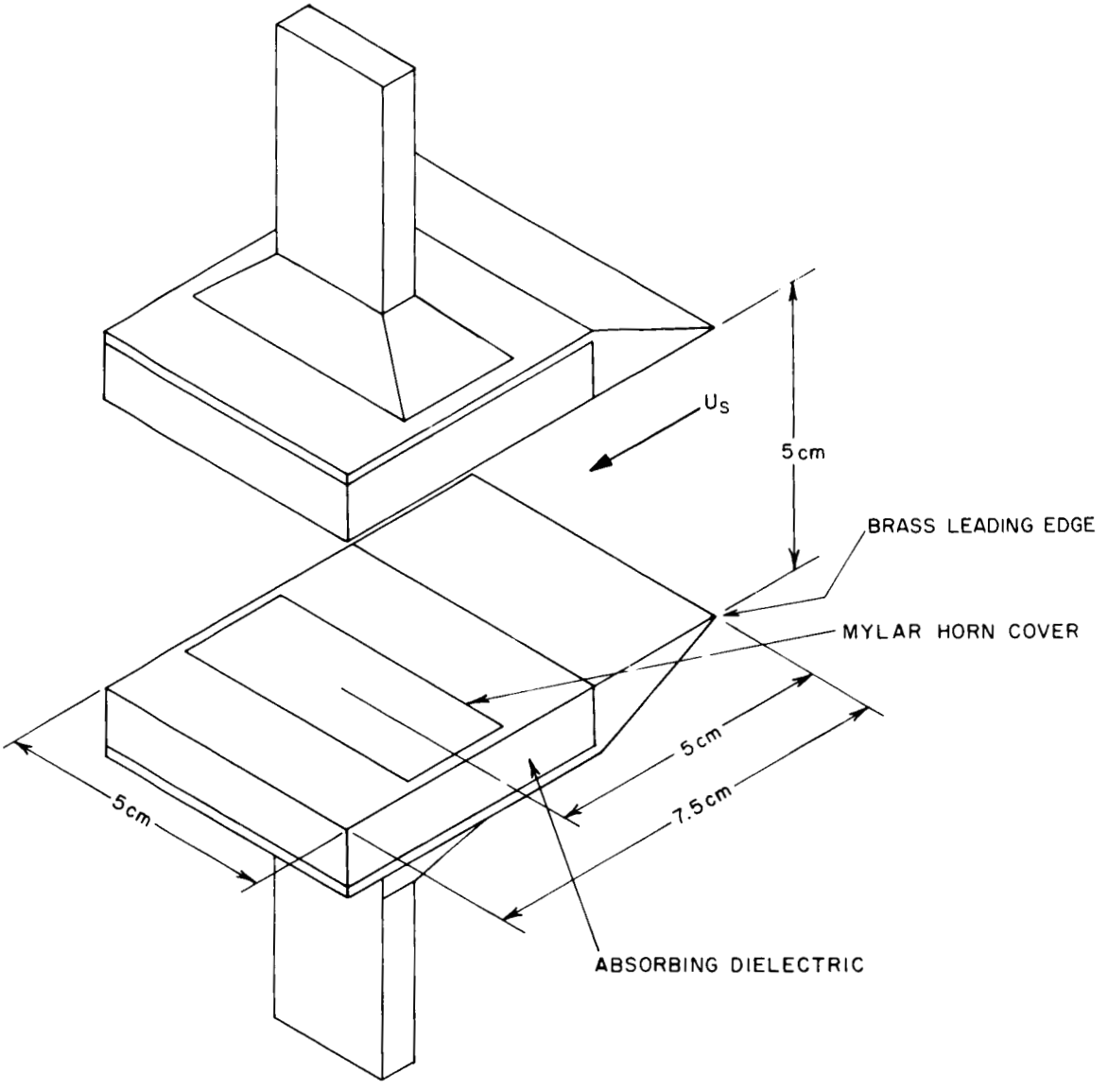

FIG. A-5 EXPERIMENTAL CONFIGURATION OF MICROWAVE INTERFEROMETER

40 shots on the tube without cleaning indicated electron densities as much as an order of magnitude lower than equilibrium. After cleaning, the interferometer still read lower electron densities than equilibrium, but the level was raised to within a factor of two of equilibrium. A 0.25 × 6.4-mm probe mounted between the interferometer plates indicated electron densities close to those deduced from the interferometer. A similar probe mounted forward of the interferometer plates indicated

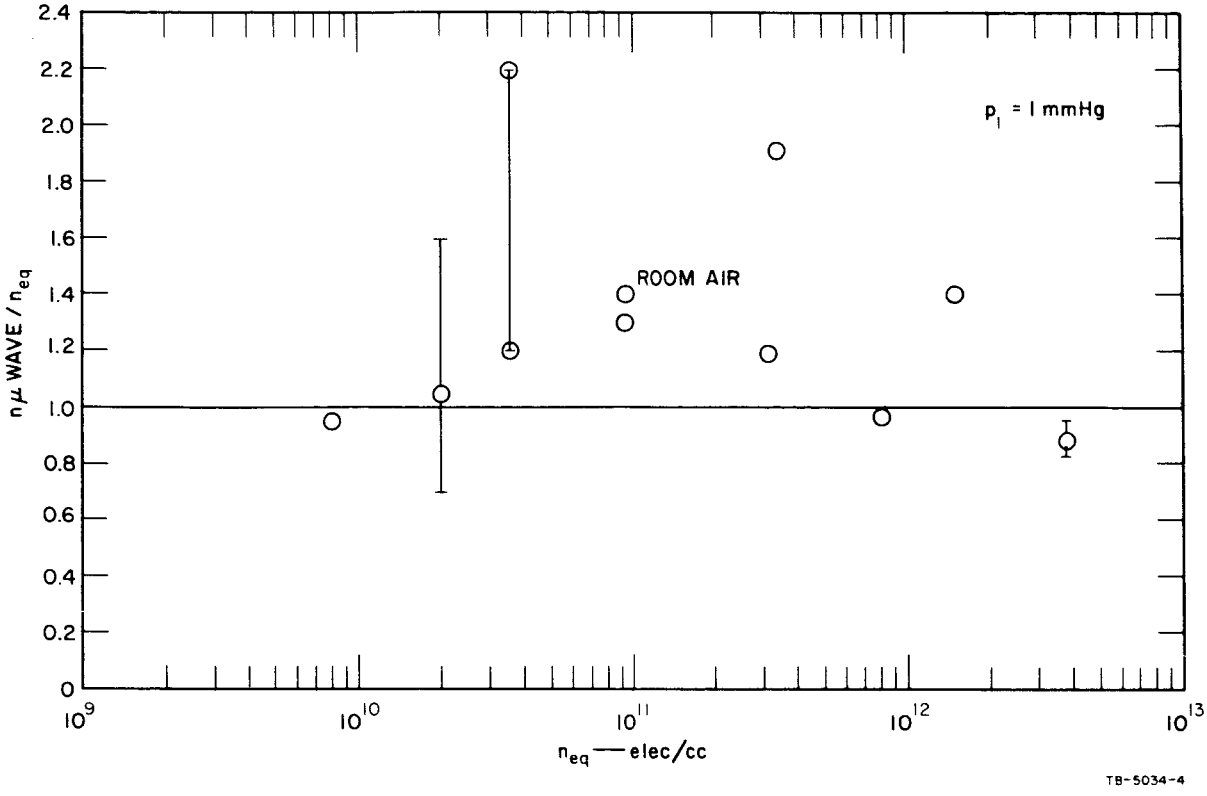

FIG. A-6 COMPARISON OF ELECTRON DENSITIES AS MEASURED BY MICROWAVE INTERFEROMETER WITH EQUILIBRIUM ELECTRON DENSITIES

electron densities higher than the probe mounted between the plates. The forward probe measured values closer to equilibrium than the probe mounted between the plates.

These results indicate that the plates were disturbing the flow at 0.1 mmHg initial pressures and causing a lower electron density to appear between the plates than exists in free stream. The free-stream electron density as measured by the forward probe indicated electron densities within a factor of two of equilibrium. The agreement between the interferometer and the probe located between the plates is taken as evidence that the 0.25-mm free-stream probe is accurately measuring the electron density.

Measurements made with the identical probes spaced 120 degrees apart around the circumference of the tube indicated that variations in electron density around the tube can be as high as a factor of two.

REFERENCES

1. I. Langmuir and H. Mott-Smith, "Studies of Electric Discharges at Low Pressures," General Electric Review **27**, Nos. 7, 8, 9, pp. 449-455, 538-548, 616-623 (July, August, September 1924).

2. D. Bohm, E. H. S. Burhop, and H. S. W. Massey, "The Use of Probes for Plasma Exploration in Strong Magnetic Fields," in Characteristics of Electrical Discharges in Magnetic Fields, pp. 13-76, Ed. Guthrie and Wakerling (McGraw-Hill Book Company, New York, New York, 1949).

3. G. Schultz and S. C. Brown, "Microwave Study of Positive Ion Collection by Probes," Phys. Rev. **98**, No. 6, pp. 1642-1649 (15 June 1955).

4. G. Hok, et al., "Dynamic Probe Measurements in the Ionosphere," Scientific Report FS-3, University of Michigan Research Institute, Reprinted under Contract AF 19(604)-1843 (November 1958).

5. J. F. Allen, R. L. F. Boyd, and P. Reynolds, "The Collection of Positive Ions by a Probe Immersed in a Plasma," Proc. Phys. Soc. (London) Sec. B 5, p. 70 (1957).

6. E. O. Johnson and L. Malter, "A Floating Double Method for Measurements in Gas Discharge," Phys. Rev. **80**, No. 1, pp. 56-68 (1 October 1950).

7. W. E. Scharfman, "The Use of Langmuir Probes to Determine the Electron Density Surrounding Re-Entry Vehicles," Final Report, Contract NAS1-2967, SRI Project 4456, Stanford Research Institute, Menlo Park, California (January 1964).

8. W. R. Hoegy and L. H. Brace, "The Dumbbell Electrostatic Ionosphere Probe: Theoretical Aspects," Scientific Report JS-1, ORA Projects 2816-1, 03484, and 03599, Space Physics Research Laboratory, University of Michigan, Ann Arbor, Michigan (September 1961).

9. F. O. Smetana, "On the Current Collected by a Charged Circular Cylinder Immersed in a Two-Dimensional Rarified Plasma Stream," Proc. Third Symposium on Rarified Gas Dynamics, Vol. II, pp. 65-91 (Academic Press, New York, New York, 1963).

10. R. E. Probstein, "Shock Wave and Flow Field Development in Hypersonic Re-Entry," ARS J., pp. 185-194 (February 1961).

11. A. J. Pallone, J. A. Moore, and J. I. Erdos, "Nonequilibrium, Nonsimilar Solutions of the Laminar Boundary-Layer Equations," AIAA J. **2**, No. 10, pp. 1706-1713 (October 1964).

12. F. G. Blottner, "Nonequilibrium Laminar Boundary-Layer Flow of Ionized Air," AIAA J. 2, No. 11, pp. 1921-1927 (November 1964).

13. J. D. Cobine, Gaseous Conductors, pp. 128-129 (Dover Publications, New York, New York, 1958).

14. T. C. Adamson, Jr., "Estimation of Nonequilibrium Reaction Flight Regimes for Blunt Bodies at Hypersonic Speeds," ARS J., pp. 358-360 (April 1960).

15. J. E. Hartsel, "A Shock Tube Study of the Blunt Body Shock Layer and Plasma Sheath Thermal Noise Emission," Ohio State University Research Foundation, Antenna Laboratory Project No. 4357, Contract AF 33(657)-10523 (March 1965).

16. S. C. Lin and J. D. Teare, "Rate of Ionization Behind Shock Waves in Air, II. Theoretical Interpretations," Phys. Fluids 6, No. 3, pp. 355-375 (March 1963).

17. J. C. Camm and P. H. Rose, "Electric Arc-Drive Shock Tube," Phys. Fluids 6, No. 5, pp. 663-678 (May 1963).

STANFORD RESEARCH INSTITUTE

MENLO PARK
CALIFORNIA

Regional Offices and Laboratories

Southern California Laboratories
820 Mission Street
South Pasadena, California

Washington Office
808–17th Street, N.W.
Washington 6, D.C.

New York Office
270 Park Avenue, Room 1770
New York 17, New York

Detroit Office
1025 East Maple Road
Birmingham, Michigan

European Office
Pelikanstrasse 37
Zurich 1, Switzerland

Japan Office
c/o Nomura Securities Co., Ltd.
1–1 Nihonbashidori, Chuo-ku
Tokyo, Japan

Representatives

Toronto, Ontario, Canada
Cyril A. Ing
Room 710, 67 Yonge St.
Toronto 1, Ontario, Canada

Milan, Italy
Lorenzo Franceschini
Via Macedonio Melloni, 49
Milano, Italy